Structural Controls and Deformation History of the Orogenic Island Gold Deposit, Michipicoten Greenstone Belt, Ontario

by

Katia Jellicoe

A thesis

presented to the University of Waterloo

in fulfillment of the

thesis requirement for the degree of

Master of Science

in

Earth Sciences

Waterloo, Ontario, Canada, 2019

© Katia Jellicoe 2019

Author's Declaration

This thesis consists of material all of which I authored or co-authored: see Statement of Contributions included in the thesis. This is a true copy of the thesis, including any required final revisions, as accepted by my examiners.

I understand that my thesis may be made electronically available to the public.

Statement of Contributions

This thesis is my own work. The following contributor is a co-author on Chapter 5: Natasha Wodicka performed the U-Pb analyses and provided the analytical techniques (Section 5.2), results (Table 1, 2), and diagrams and zircon images (Figures 5.1, 5.2, 5.3, 5.4).

Abstract

Island Gold is a currently producing mine on the high-grade orogenic Island Gold deposit in northern Ontario. It is located within the southern domain of the regional Goudreau Lake Deformation Zone (GLDZ), which trends east-west through the Michipicoten greenstone belt of the Wawa-Abitibi terrane.

The study area encompasses the Island Gold deposit and is located along the northern limb of the Goudreau Anticline, a regional-scale fold attributed to D1 deformation. D2 consists of regional greenschist-facies metamorphism, camp-scale F_2 folds, associated steep axial-planar foliation S_2, moderately to steeply east-plunging stretching lineation L_{2a}, and sub-horizontal slickenside striations L_{2b}. D_3 structures are camp- and outcrop-scale F_3 folding, which deforms S_2 foliation into shallowly-plunging Z-folds, weakly developed axial-planar cleavage S_3, and brittle reverse faults. The Island Gold deposit forms a mineralized corridor south of the trondhjemitic Webb Lake Stock intrusion. The main Lochalsh, Island, Island Deep, and Extension 1 and 2 Zones consist of steeply dipping, subparallel ore zones of laminated V1 quartz veins and V2 veinlets within a silicic-sericitic alteration package. V3 conjugate quartz-carbonate extensional veins cross-cut V1 and V2 ore veins. Offset to the north of the main zones is the Goudreau Zone, which contains both sub-vertical and sub-horizontal ore zones with V_{GD} ore veins. All pre-existing vein sets and structures were overprinted by V4 tourmaline veins. U-Pb zircon geochronology analyses from this study place the age of the mineralized Webb Lake Stock at 2724.1±4.3 Ma and the age of the post-mineralization I2M intrusion at 2672.2±3.5 Ma, which constrain the upper and lower absolute limits on timing of mineralization. Youngest detrital zircon ages from the overlying Doré metasedimentary rocks, which show D2 greenschist-facies metamorphism, further constrain this timing to between 2680±3 Ma and 2672.2±3.5 Ma.

The GLDZ formed during D_2 deformation along a major lithologic contact. The Island Gold deposit V1 and V2 ore veins were emplaced sub-parallel to S_2 foliation along a strain shadow created by the Webb Lake Stock during D2 north-side-up, sinistral transpression. Subsequent D_3 deformation folded and sheared the ore zones and V3 veins were emplaced in areas of high competency contrast.

Acknowledgements

I would like to thank my supervisor, Dr. Shoufa Lin, for giving me the opportunity to work on such an amazing project, as well as for his support, encouragement, and insights throughout this process. I am also incredibly grateful for my committee: Dr. Chris Yakymchuk, for providing guidance, support, and valuable feedback; and Dr. Brian Kendall, for demystifying radiogenic isotope systems.

My field work was made possible by the expertise and assistance of the staff at the Island Gold Mine and I would like to thank them for their support, which continued well beyond my summers spent on site. Thank you especially to: Doug MacMillan and Harold Tracanelli, for sharing their time and vast exploration knowledge; Raya Puchalski, Hélène Mellier, Simon Comtois-Urbain, Jessica Morris, and the rest of the geology department, for discussions and technical assistance; and the P.T., for keeping me focused.

The GSC provided technical and financial support, but also the invaluable experience of spending time in the field and in discussion with their geologists. Thank you to Patrick Mercier-Langevin for patiently facilitating and encouraging during this project.

I couldn't have done this without the love and support of my family and friends. So much love and gratitude go to Brent Jellicoe, Ruth Jellicoe, Jeff Mann, Ben Jellicoe, Alixaya Jellicoe, Brad Larson, Murphie Jellicoe, and Emily Lafreniere. The friends that I met at the University of Waterloo will always hold a special place in my heart and I can't possibly thank them all as much as they deserve. Thank you to Jen Parks for your unwavering friendship, encouragement, and kindness; to Martha Merrall and Paula Parejo for the love and support that started as soon as I arrived in Waterloo; to Alex Krapf-Jones for endless discussions on geology and life; and to the incredible group of grad students and beyond that became my second family. Finally, this experience would not have happened without the friends and mentors I met during my undergrad at the University of Saskatchewan, particularly Dr. Kevin Ansdell and Dr. Victoria Stinson.

Table of Contents

List of Figures

List of Tables

1. Introduction

1.1 Scope and purpose

Significant gold mineralization occurs along the Goudreau Lake Deformation Zone within the Michipicoten greenstone belt and numerous mines have operated in the area in the last century. The Island Gold deposit is a high-grade, lode-gold deposit located along the Goudreau Lake Deformation Zone. Goudreau Lake lies above where the deposit would outcrop, and as such the Island Gold deposit was not discovered until much later than other deposits in the area. Studies in the Michipicoten greenstone belt have been conducted by government surveys beginning in the early 1900s (Bruce, 1940; Goodwin, 1962) up until the early 1990s, but the Island Gold deposit was only just beginning to be developed at the time of the last detailed study in the area (Heather and Arias, 1992) and was not yet accessible for closer observation. The Island Gold mine has now been in production for over ten years and presents a unique opportunity to study the deposit and the surrounding Goudreau Lake Deformation Zone from both the surface and extensive underground workings. Mineralization is still open laterally and at depth, but an improved understanding of the deposit and its tectonic setting is however necessary to optimize exploration at the mine and elsewhere in the district.

The objectives of this study are (1) establish and characterize the generations of deformation in the study area; (2) constrain the relative and absolute timing of deformation events and mineralization; and (3) determine the structural controls on mineralization.

To achieve these objectives, camp- and outcrop-scale field mapping was carried out to document structures and cross-cutting relationships within the study area to

determine the deformation history. Underground mapping at the Island Gold mine and petrographic analysis were used to identify and characterize vein generations, which were then correlated to generations of deformation. Samples were collected where possible for both thin section analysis and for fire assay to determine gold content. Selected intrusions were sampled for U-Pb geochronology to constrain the absolute timing of deformation and mineralization.

1.2 Location, access, and topography

The study area of this thesis is located in northern Ontario, approximately 16 km southeast of the town of Dubreuilville and in the southeast corner of Finan township. It occupies an area of roughly 22 km^2 with the UTM coordinates (NAD 83, Zone 16N) of 5,350,000N – 5,353,700N and 687,300E – 693,500E (Figure 1.1).

Access to the study area is available by road year-round. Highway ON-519 E, off of Trans-Canada Hwy/ON-17 N, is paved and provides access to the town of Dubreuilville. An unnamed dirt and gravel road, maintained by the company, connects Highway ON-519 E near Dubreuilville to the Goudreau Road, which runs through the study area. Branching off from Goudreau Road within the study area are multiple recent drill-access roads and historic logging roads. Most are traversable by truck or ATV.

Local topography is typical of Canadian shield, with low to moderate exposure of low-profile bedrock interspersed with glacial sediments, heavily wooded areas, muskegs, and lakes.

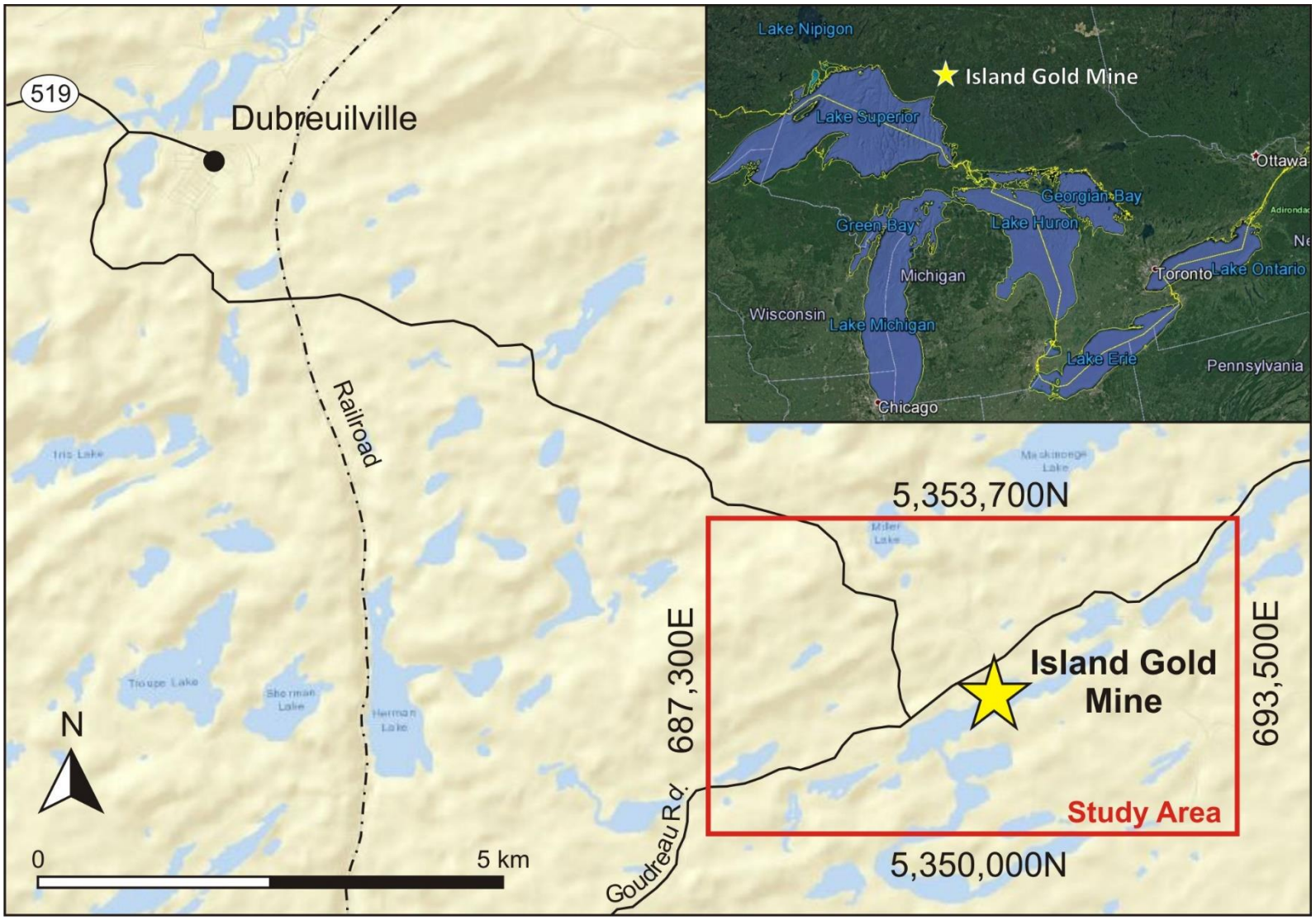

Figure 1.1: Geographic location of the study area. UTM co-ordinates are in NAD 83, Zone 16N.

2. Geology of the Michipicoten greenstone belt

2.1 Previous work

The Michipicoten greenstone belt has been of economic interest since the early 1900s, when iron and gold were discovered near Wawa, Ontario. Early mapping in the Michipicoten greenstone belt was completed by E.L. Bruce in the late 1940s, and since then the area has been the subject of multiple mapping projects (Goodwin, 1962, 1964; Sage, 1987, 1993, 1994; Heather and Arias, 1987, 1992; McGill, 1992; and others) to elucidate the geological and deformational history as well as assess the economic potential of the area. The Goudreau-Lochalsh area of the belt was first targeted for iron ore, but the discovery of gold occurrences spurred further exploration and led to the discovery of multiple deposits in the area.

Mapping of the Michipicoten greenstone belt by Goodwin (1962) initially described three volcanic cycles, three major east-west trending folds later folded by three major northeast trending folds, and multiple north-striking sinistral faults. A ten-season, systematic mapping program was undertaken by the Ontario Geological Survey from 1979 to 1988 to study the central portion of the Wawa terrane and produced multiple 1: 15,840 scale maps of over fifteen townships, as well as accompanying reports and geochemical analyses (Sage, 1994). Work by Sage (1987) documented the previously unrecognized Hawk assemblage and mapping by McGill and Shrady (1988) in the Chabanel Township identified an abrupt reversal of younging direction within a sedimentary belt and multiple fault-bounded lithologic packages, as well as an apparent fault separating the sedimentary belt from the northern volcanic terrane. These observations led to the interpretation of a thrust-imbricated sequence of volcanic and

sedimentary rocks. The recognition of a large-scale recumbent fold and the repetition of volcanic cycles along imbricate thrust-faults by Arias and Helmstaedt (1990) reorganised the stratigraphic interpretation into the current configuration (Figure 2.2). Work by Arias and Heather (1987) identified two major northeast-trending deformation zones in the Goudreau-Lochalsh area: the Goudreau Lake Deformation Zone and the Cradle Lake Deformation Zone (Figure 2.4).

Economic activity in the Goudreau-Lochalsh area began in 1916 with the development of the Morrison No. 1 iron-sulphide property by Algoma Ore Properties Ltd., and the discovery of gold within the deposit in the later years led to further gold exploration in the area by various companies. By the late 1980s, the Canamax Resources had completed extensive work on their Kremzar and Island Gold projects, and in 1988 the Kremzar mine began commercial production. The mine operated until 1990, when all operations were suspended at both the Kremzar and Island Gold projects. In 1996 Patricia Mining Corporation took over the property, and in 2003 they entered a joint venture agreement with Richmont Mines to continue exploration and development of the Island Gold project. In 2007 Richmont Mines acquired full ownership of the project and brought the Island Gold mine into commercial production the same year. Since that time, exploration to expand the resource along strike and down dip has continued with surficial and underground exploration and diamond drilling. Most recently, the property was purchased by Alamos Gold in 2017.

2.2 Tectonic framework of the Wawa subprovince

The Superior Province is a massive craton that formed during the Archean (Figure 2.1). Five discrete accretionary events are interpreted to have formed the

Superior Province and are known collectively as the Kenoran Orogeny (Card, 1990). Accretion began with the collision of the Northern Superior superterrane and North Caribou superterrane in the Northern Superior Orogeny at 2.72 Ga and continued southward for the next 40 million years (Percival et al., 2012). The Wawa-Abitibi terrane was the fourth of five terranes to join the Superior superterrane during the Kenoran Orogeny. The terrane has been interpreted as originating along a converging plate margin and shows lateral variation from immature to mature island arc rocks (Sylvester et al., 1986), and was accreted to the Superior superterrane in the Shabandowanian Orogeny which began at ca. 2.695 Ga. The cessation of arc-related magmatism and the emplacement of sanukitoid intrusions in the Wabigoon-Winnipeg River terrane at this time suggest north-verging subduction, as well as the possibility of slab break-off (Lin and Beakhouse, 2013). A similar series of events (cessation of arc magmatism, emplacement of sinuktoid intrusions) occurred within the Wawa-Abitibi terrane at 2.68 Ga with the accretion of the Minnesota River Valley terrane to the Superior superterrane in the fifth and final accretionary event, the Minnesotan orogeny, followed by cratonization (Percival et al., 2006). Cratonization began in the northern Superior Province at 2.68 Ga and continued south across the province until 2.60 Ga and was characterized, in part, by regional metamorphism, granitic plutonism, deposition of Timmiskaming-type sediments, and gold localization (Percival et al., 2012). The emplacement of granitic plutons under and into the volcanic sequences, combined with post-plutonism deformation, created synclinal keels throughout the Superior Province which gives many of the greenstone belts their current, somewhat linear, configuration (Lin and Beakhouse, 2013). The Superior Province has remained relatively tectonically stable since 2.60 Ga.

2.3 Geology and structure of the Michipicoten greenstone belt

The Michipicoten greenstone belt is composed of three bimodal volcanic assemblages ranging from late Mesoarchean to Neoarchean in age (Heather & Arias, 1992). The volcanic assemblages are overlain by the Doré metasedimentary rocks (Figure 2.3). The supracrustal rocks of the belt are regionally metamorphosed to greenschist facies and reach the amphibolite facies in contact aureoles of the surrounding plutonic rocks. Paleoproterozoic Matachewan diabase dykes pervasively intrude the greenstone belt, typically in a roughly N-S orientation.

2.3.1 Hawk Lake assemblage

The Hawk Lake assemblage is the oldest of the volcanic assemblages in the Michipicoten greenstone belt with a zircon U-Pb age of 2889.2±9.2 Ma of felsic volcanic rocks (Turek, 1988, 1992). It is poorly exposed and only found along the southern edge of the belt (Figure 2.3). The base of the Hawk Lake assemblage consists of basaltic and peridotitic komatiites which occur as pillows and massive flows. The mafic volcanics are overlain by intermediate to felsic volcanic tuffs and breccias and the assemblage is capped by a chert-magnetite-sulphide iron formation (Sage, 1994).

2.3.2 Wawa assemblage

The Wawa assemblage unconformably overlies the Hawk Lake assemblage and occurs in bands throughout the greenstone belt (Figure 2.3). It is composed of tholeiitic mafic to intermediate volcanics in the bottom portion, intermediate to felsic volcanics in the upper portion, and is capped by the Michipicoten Iron Formation. U-Pb zircon geochronology of the upper portion of the assemblage gives ages ranging from 2749 ±2 Ma to 2728.8 ±2.7 Ma (Turek, 1982; 1992).

2.3.3 Catfish assemblage

The Catfish assemblage is the youngest volcanic package in the Michipicoten greenstone belt. It overlies the Wawa assemblage, but contacts between the two have been extensively sheared and are not considered primary. Volcanics of the Catfish assemblage are of tholeiitic mafic to intermediate composition in the lower portion of the assemblage, and intermediate to felsic in the upper portion. Unlike the Hawk and Wawa, the Catfish assemblage is not capped by its associated iron formation; the Dreany Iron Formation occurs between the mafic and the felsic portions of the assemblage (Figure 2.2) (Sage, 1994). Samples from the upper portion of the assemblage gave zircon U-Pb ages of 2710±7.7 Ma and 2701±7.7 Ma (Smith, 1981; Turek, 1984).

2.3.4 Doré metasediments

The Doré metasediments are the youngest supracrustal rocks in the Michipicoten greenstone belt and occur as three belts (Figure 2.3). The southern sedimentary belt occurs near Wawa and the U-Pb age obtained from a boulder within a conglomerate unit indicates sedimentation occurred after 2698±2 Ma (Corfu and Sage, 1992). The youngest detrital zircon from the central sedimentary belt has a U-Pb age of 2682±3 Ma (Corfu and Sage, 1992). The northern sedimentary belt flanks the northern edge of the Michipicoten greenstone belt and with the youngest detrital zircon dated has a U-Pb age of 2680±3 Ma (Corfu and Sage, 1992). Doré metasediments typically unconformably overlie the Catfish and Wawa assemblages, but they have also been recorded as interfingering with the felsic to intermediate volcanics of the Catfish assemblage. This relationship has been attributed to a period of intermediate to felsic volcanism and

sedimentation that occurred simultaneously (Rice & Donaldson, 1992; Sage, 1993, 1994), but may actually be the result of tectonic juxtaposition.

Metamorphism within the Doré metasediments is mostly of greenschist grade and reaches lower amphibolite grade in areas of contact metamorphism from plutons (Rice and Donaldson, 1992).

2.3.5 Goudreau Lake Deformation Zone

The Goudreau Lake Deformation Zone (GLDZ) is a regional structure composed of multiple shear zones. It is located near the northern edge of the Michipicoten greenstone belt, reaching approximately 4.5 km in width and has been traced along strike for over 25 km and strikes 070° to 100°. The deformation zone is centred on the contact between two volcanic assemblages. The GLDZ has been divided into four domains (North, East, South, and West) (Figure 2.4) based on location and deformation style (Arias and Heather, 1987). The control of initial deformation is attributed to the lithological contact between felsic metavolcanics in the south and mafic metavolcanics to the north (Arias and Heather, 1987).

The Southern Domain of the Goudreau Lake Deformation Zone (GLDZ) is located within felsic rocks of the Wawa assemblage. It is approximately 2 km wide and has been traced for 8 km along strike. It strikes 070° and consists of subparallel, brittle-ductile shears (Arias and Heather, 1987). Two regional brittle fault zones trending at 135-145° may bound or offset the Southern Domain (Heather and Arias, 1987): the McVeigh Creek fault to the west, and the Maskinonge Lake fault to the east.

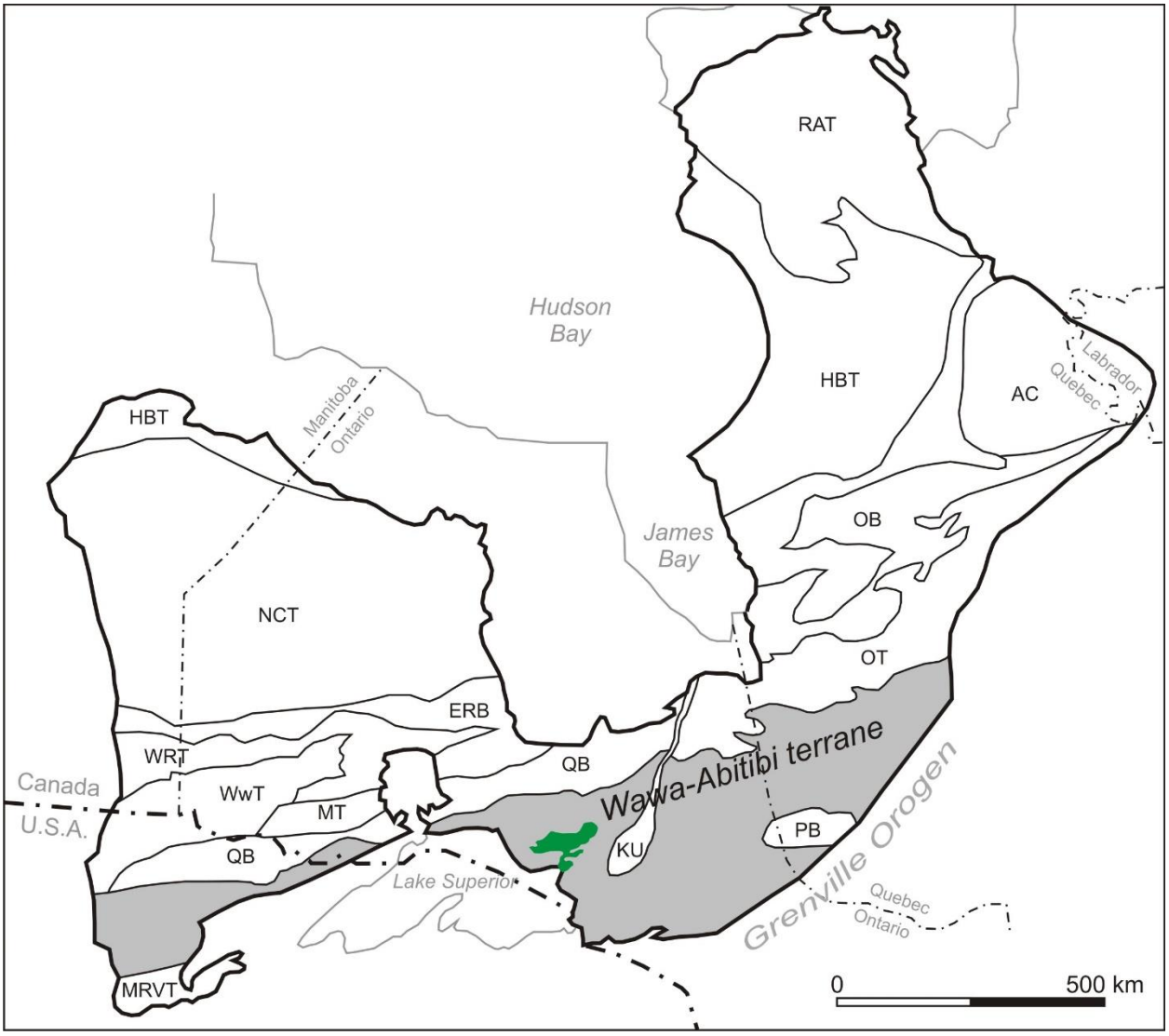

Figure 2.1: Simplified map of the Superior Province (bold outline) with terranes and belts. Note the Wawa-Abitibi terrane highlighted in grey and the location of the Michipicoten greenstone belt (green). AC=Ashuanipi complex; ERB=English River belt; HBT=Hudson Bay terrane; KU=Kapuskasing uplift; MRVT=Minnesota River Valley terrane; MT=Marmion terrane; NCT=North Caribou terrane; OB=Opinaca belt; OT=Opatica terrane; PB=Pontiac belt; QB=Quetico belt; RAT=Riviére Arnoud terrane; WRT=Winnipeg River terrane; WwT=Western Wabigoon terrane. With minor modifications from Percival et al., 2012.

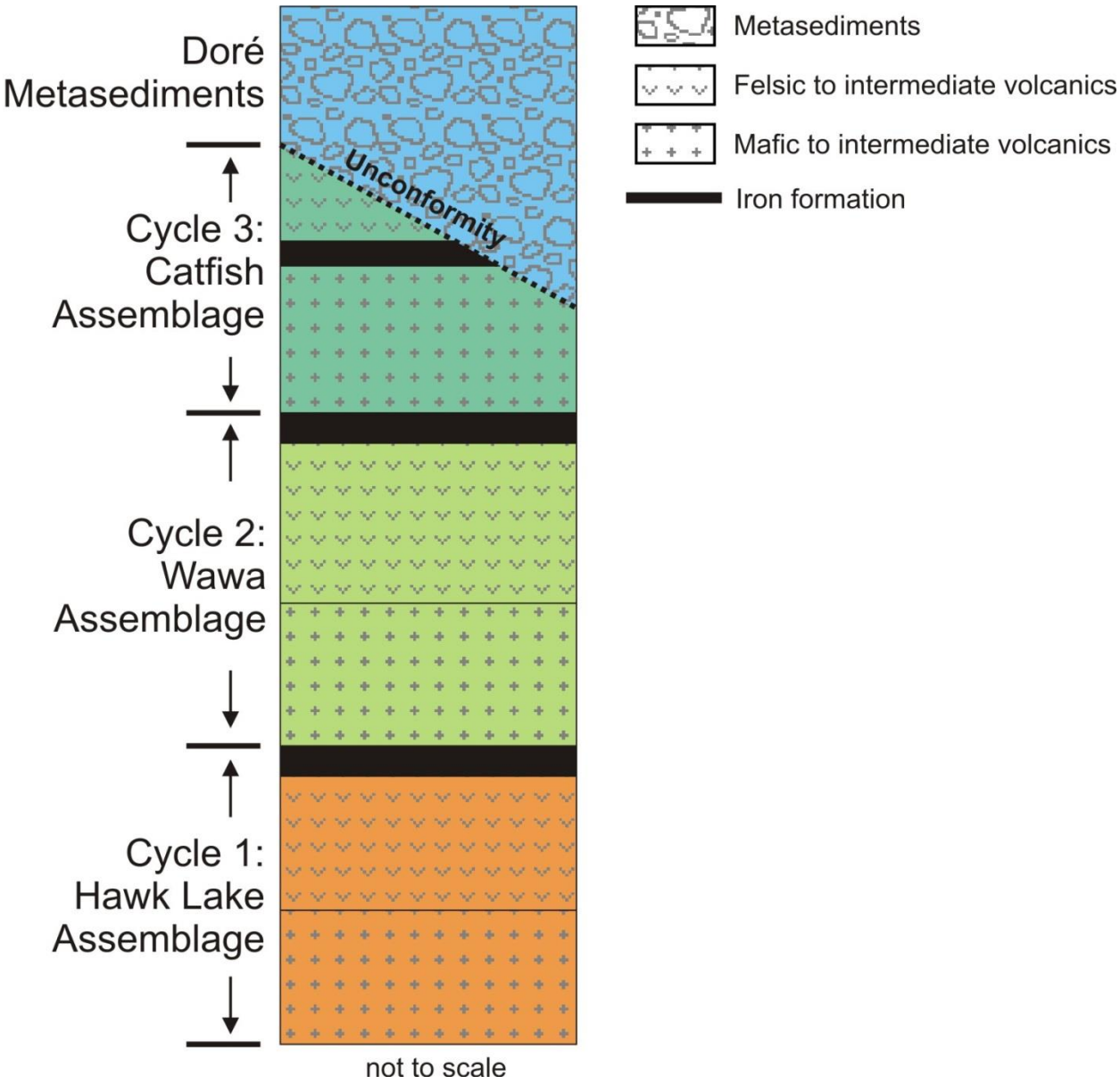

Figure 2.2: Stratigraphic column of the volcanic and sedimentary rocks of the Michipicoten greenstone belt. Modified from Arias and Helmstaedt, 1990

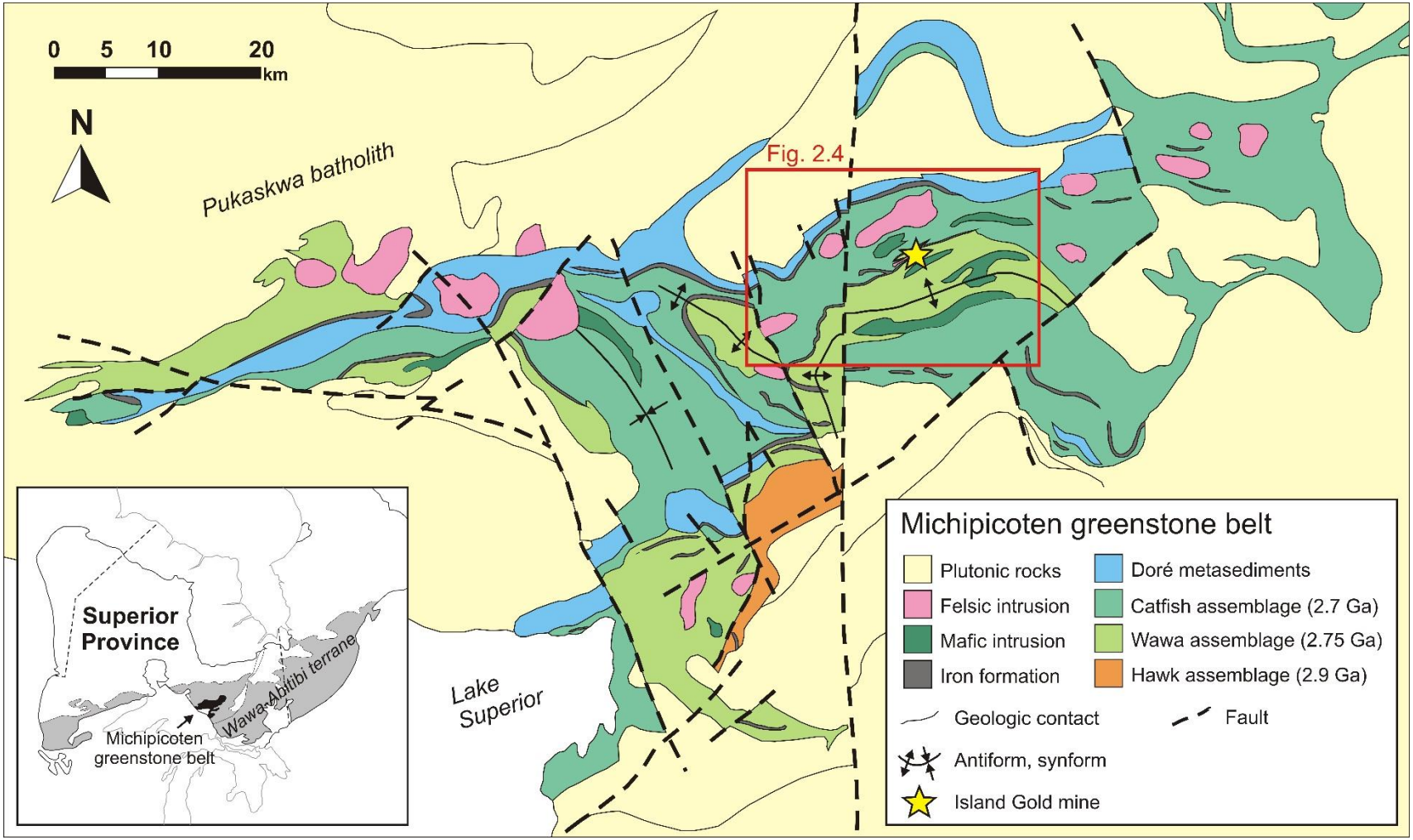

Figure 2.3: Simplified geological map of the Michipicoten greenstone belt showing the distribution of volcanic assemblages and the location of the Island Gold mine. Area of Figure 2.3 and the location of the Goudreau Lake Deformation Zone is indicated by the red box. Modified from Williams et al. (1991). Location of the Michipicoten greenstone belt highlighted in inset map of the Superior Province. Modified from Card (1990).

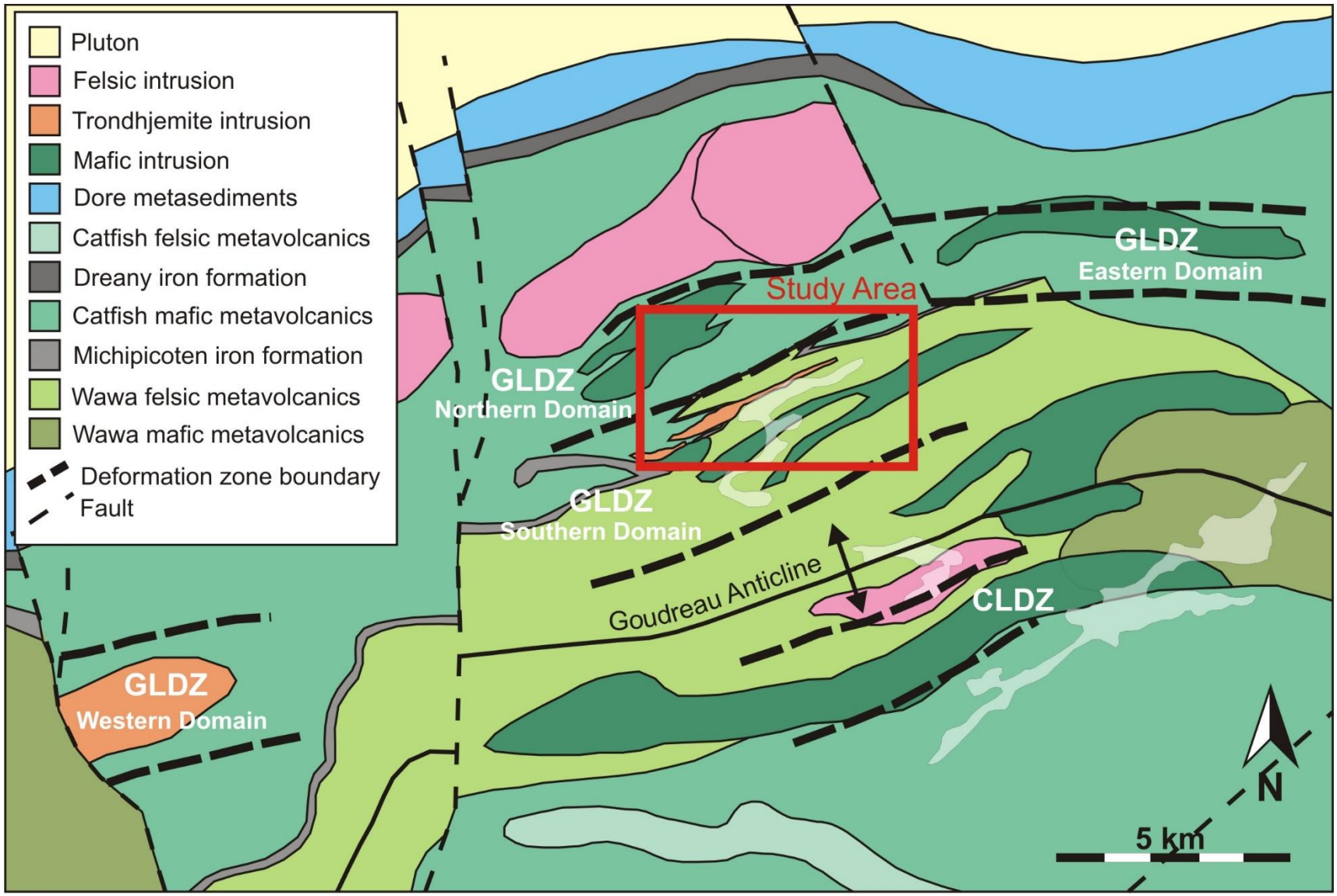

Figure 2.4: Simplified geological map showing the location and geometry of the Goudreau Lake Deformation Zone. Location of the study area outlined by red box. Modified from Arias & Heather (1987). GLDZ=Goudreau Lake Deformation Zone; CLDZ=Cradle Lake Deformation Zone.

3. Geology and structure of the Island Gold Deposit in the Southern Goudreau Lake Deformation Zone

3.1 Introduction

The study area encompasses a section of the contact between the ~2750 Ma Wawa assemblage and the overlying ~2700 Ma Catfish assemblage (Figure 3.1).

3.2 Geology of the Study Area

3.2.1. Wawa assemblage

The intermediate to felsic volcanics of the younger, or "upper", phase of the Wawa assemblage occupy the southern half of the study area and consist primarily of dacitic quartz-feldspar phenoclastic tuff, with lesser occurrences of lapilli tuff and tuff breccia that have all been metamorphosed to greenschist facies. In relatively undeformed tuff, the quartz-feldspar phenocrysts are euhedral to subhedral and weather to a light cream colour (Figure 3.2a) while the finer-grained matrix commonly weathers to a medium- to light-green. Where the tuff has been deformed the phenocrysts are flattened to varying degrees and define the foliation (Figure 3.2b).

Capping the intermediate to felsic volcanics of the Wawa assemblage is the Michipicoten Iron Formation, locally referred to within the study area as the Morrison No.1 Iron Range. Highly deformed banded iron formation is exposed south of the Magino mine, while at the Morrison No.1 exposure south of the Island Gold mine portal, the iron range occurs as massive pyrite with minor chert and contains cobbles of volcanic material.

3.2.2 Catfish assemblage

The mafic to intermediate volcanics of the older, or "lower", phase of the Catfish assemblage occupy the northern half of the study area and locally consist of massive flows that have been metamorphosed to greenschist facies. They are fine-grained and weather to a medium green with occasional rust-coloured alteration (Figure 3.2c). Large mafic intrusions have also been documented within the mafic volcanics of the Catfish assemblage. Historically these intrusions have been identified during mapping primarily by grain size, but due to extensive alteration this classification is not always accurate.

3.2.4 Webb Lake Stock

The Webb Lake Stock is a sheet-like trondhjemitic intrusion that crosscuts the contact between the upper Wawa assemblage and the lower Catfish assemblage where it is folded in the study area. On fresh surfaces the trondhjemite is a mottled grey-green which weathers to a creamy yellow (Figure 3.2d). It is medium- to fine-grained and equigranular, and on both fresh and weathered surfaces the characteristic millimetre-sized, rounded, blue-grey quartz grains are readily apparent. The surface trace of the stock is subparallel to regional stratigraphy and dips steeply to the north. The width of the stock varies from 150m to 300m and the long axis extends beyond the study area to the east. In the area of the Magino mine, the Webb Lake Stock has been mapped as two bodies; divided into a north and south body by either a fine-grained intrusion or a sheared zone. The northern contact of the Webb Lake Stock is irregular and interfingers with aureole rocks, while the southern contact is relatively straight and highly sheared. The Magino mine is located in the northern body of the Webb Lake Stock and

mineralization occurs within a stockwork of “shear-fracture-hosted” quartz veins (Heather & Arias, 1992). The southern body is not mineralized.

3.2.5 “I2M” Intrusion

The “I2M” is an unmineralized intrusive body that cross-cuts Island Deep ore zones. It is medium- to fine-grained, mottled grey and pink and contains elongated phenocrysts of chlorite and biotite with accessory blocky pyrite (Figure 3.2e). Petrographic study indicates that the I2M is a nepheline-bearing monzonite with only minor deformation (T. Ciufo, 2019). The I2M is 2-4 metres wide where it crosses the mine workings at the 740 level and dips steeply north.

3.2.6 Matachewan Diabase Dykes

Proterozoic Matachewan diabase dykes intrude all Archean assemblages. Within the study area they appear as relatively “fresh”-looking dark green intrusions (Figure 3.2f) less than 50 m wide that are subvertical and trend NW-SE (Figure 3.1). Offset of older units and structures is observed along the dykes.

3.2.7 Island Gold deposit

The Island Gold deposit is hosted in the volcanics of the upper Wawa assemblage. The deposit is comprised of the Island Gold, Island Deep, Lochalsh, and Extension 1 and 2 Zones, which lie along the same strike, and the Goudreau Zone which lies to the north (Fig. 3.1).

Ore zones consist of millimetre- to decimetre-wide auriferous quartz veins enveloped by an alteration package referred to at the mine as “API” (Alteration Package Island). API is pervasive carbonate and silica alteration that gives the host rocks a

bleached, grey-beige appearance. In zones of intense alteration, pre-existing rock textures or fabrics are often obliterated.

The Lochalsh, Island, and Extension Zones form a mineralized corridor that widens from 50 m near surface to over 100 m at depth. The zones are hosted in intermediate to felsic metavolcanic rocks and consist of sub-parallel, metres-wide ore zones with an average strike of 070° and average dip of 80° to the south, and ore shoots plunging moderately to the northeast. At approximately 500 m depth there is a "flexure" in the zones where the dip shallows to the south before steepening again. This flexure separates the main Island Zone vertically into the Island Gold Zone above the flexure and the Island Deep Zone below. The ore zones within the Island Zone are labelled, from south to north, as the G1, G, B, C, D, D1, E, and E1 zones (Figure 3.3; Figure 3.4). An anastomosing relationship, documented during mining operations, exists between the ore zones. The C and D zones merge to form the C/D zone; the E and E1 zones merge to form the E1E zone; and at depth the D1 zone merges in and out of the E1E zone. The C zone is the most continuous and consistently of high-grade of these ore zones and is the main economic target. Within the Extension 1 and 2 zones the E1E ore zone is the main economic target.

The Goudreau Zone lies immediately south of the Webb Lake Stock (Figure 3.1). It is hosted by both intermediate to felsic volcanic rocks and the Webb Lake Stock and dioritic intrusions and consists of several steeply dipping ore zones, similar to the Island Zones, as well as sub-horizontal ore zones (Figure 3.5) consisting of tightly folded sub-horizontal ore veins. Intersections in this zone can be very high grade but are less consistent than those found in the main Island zones.

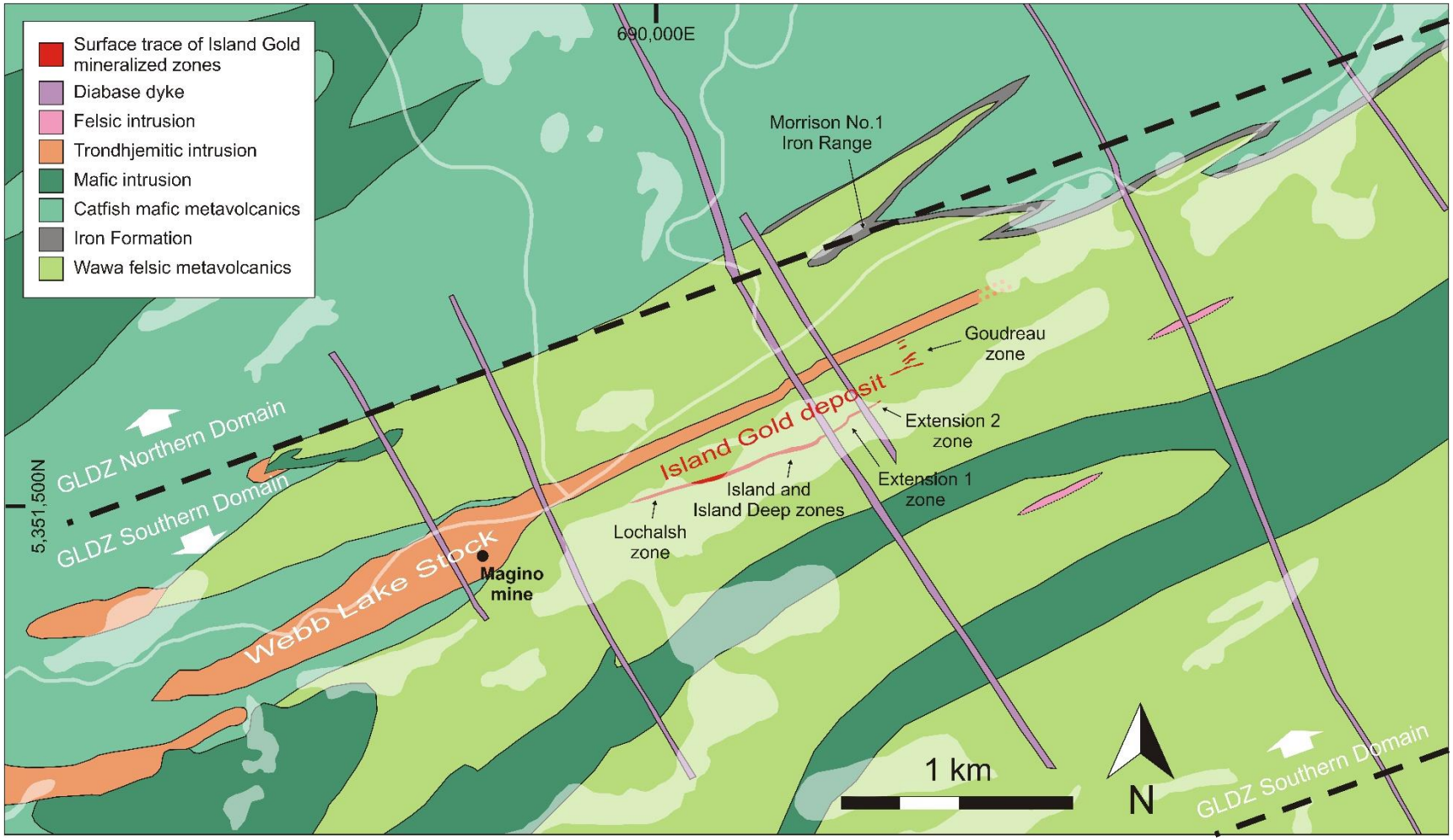

Figure 3.1 Geological map of the study area showing the southern Goudreau Lake Deformation Zone boundaries and the Island Gold deposit zones. Note the location of the Island Gold deposit relative to the Webb Lake Stock trondhjemitic intrusion. Modified from mapping by the Island Gold mine and Magino mine.

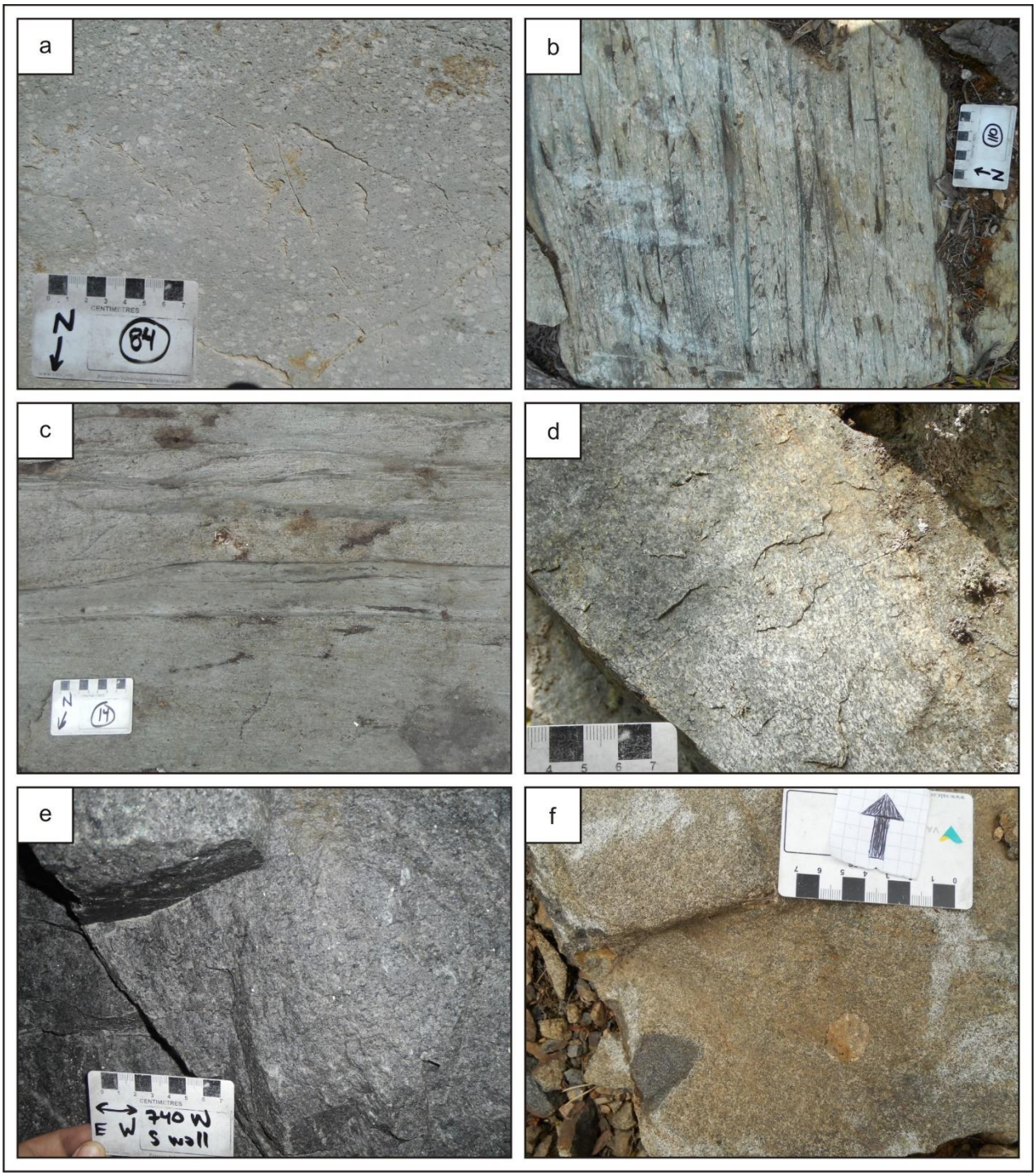

Figure 3.2: Outcrop photographs of the main lithologies found in the study area. a) Relatively undeformed dacitic tuff from the Wawa assemblage. b) Foliated dacitic tuff from the Wawa assemblage. c) Mafic volcanics from the Catfish assemblage. d) Webb Lake Stock trondhjemitic intrusion. e) "I2M" monzonite intrusion, f) diabase dyke.

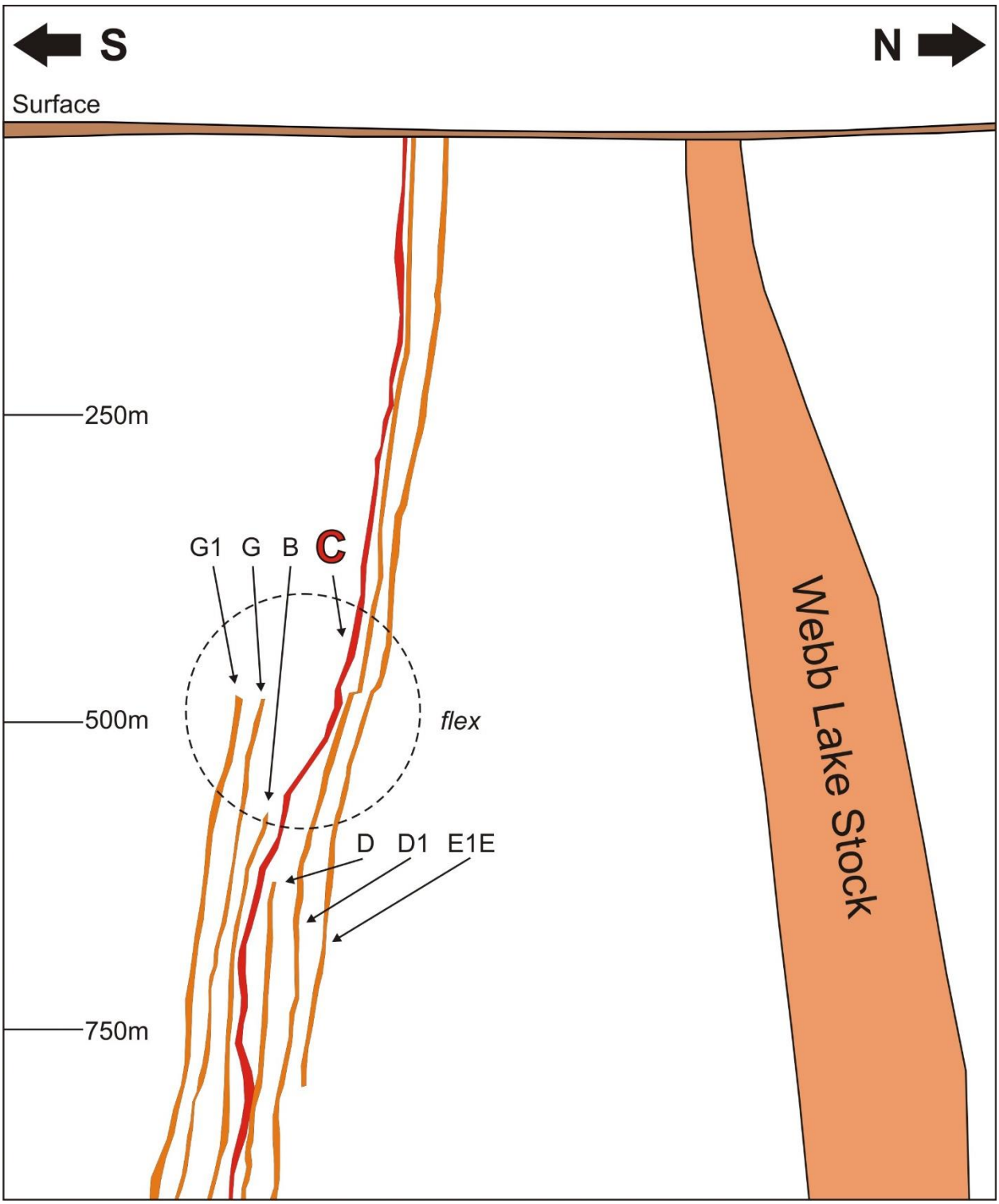

Figure 3.3: Generalized cross-section through the Island Zone (above 500m depth) and Island Deep Zone (below 500m depth) showing the spatial geometry of the ore zones and the Webb Lake Stock. Letters correspond to ore zones (in orange), with the C-zone highlighted in red. Note the "flex" in the ore zones outlined by the dashed circle. Redrawn with minor modifications after a diagram from the Island Gold mine.

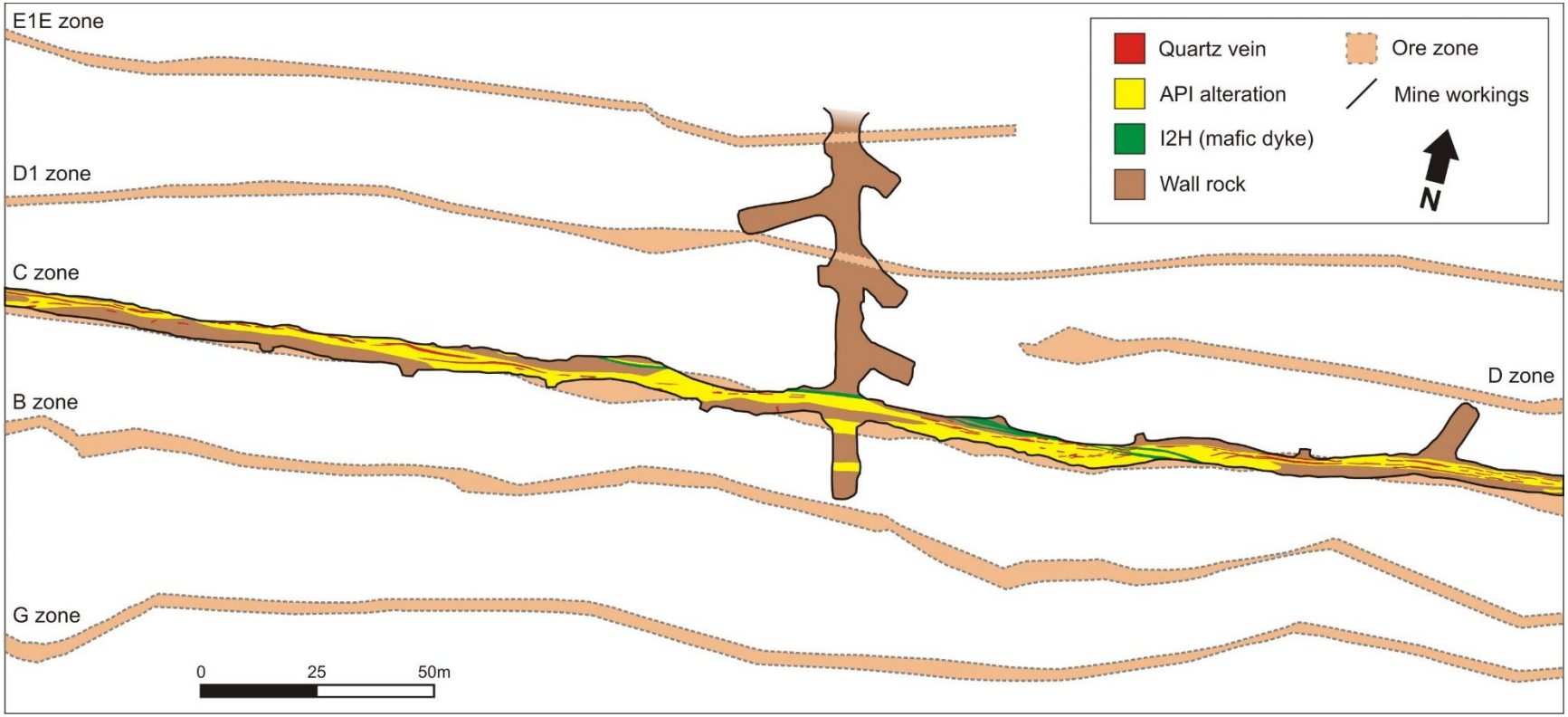

Figure 3.4: Plan-view of the 635-level in the Island Deep Zone of Island Gold mine showing the arrangement of sub-parallel ore zones. Note the I2H intrusion (in green) crossing through the C-zone mineralization (in yellow). Redrawn with minor modification after a mine level plan and geological back-mapping from the Island Gold mine.

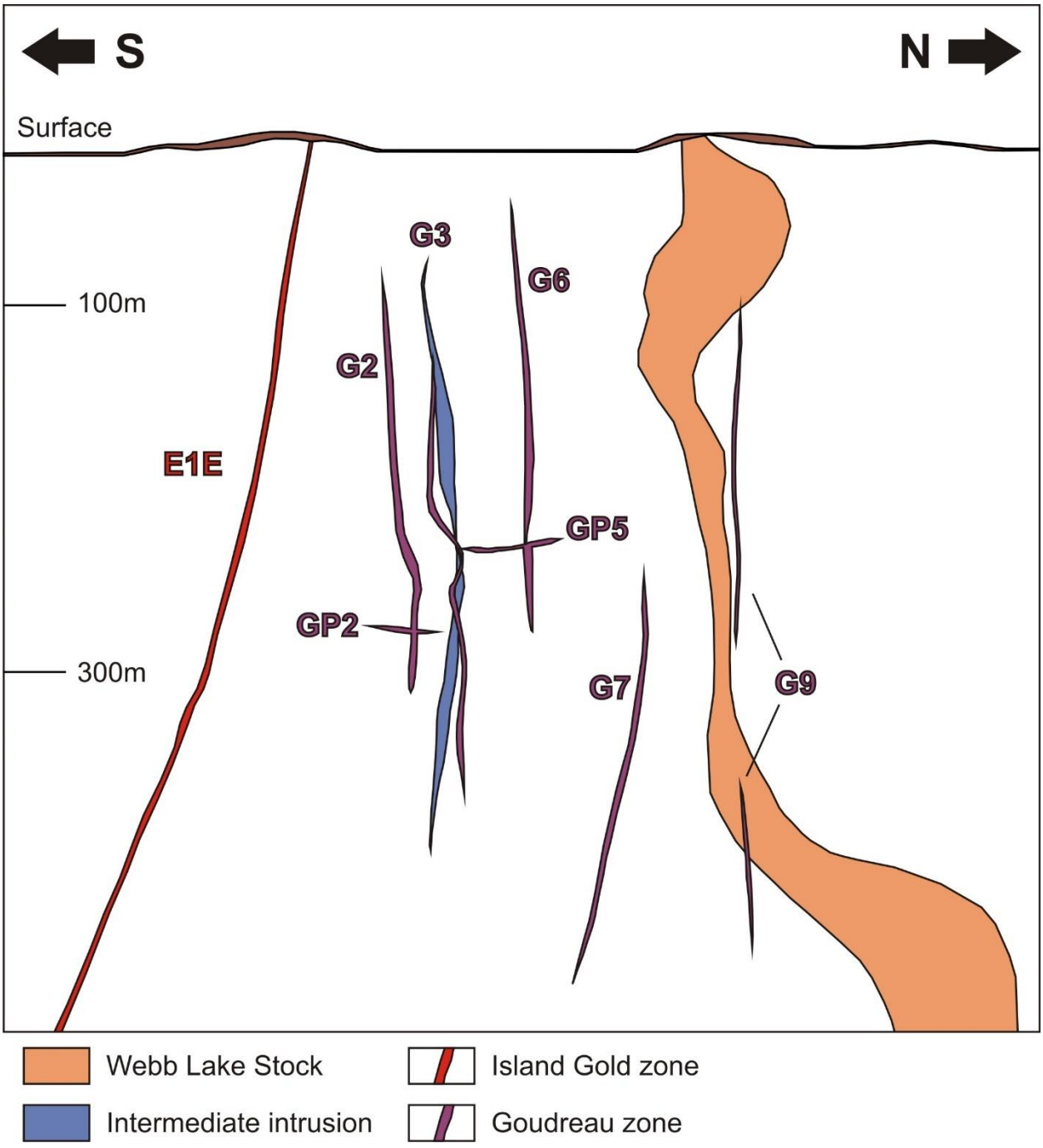

Figure 3.5: Vertical section 15800E (Island Gold mine grid, looking west) through the Goudreau Zone showing arrangement of ore zones and the spatial relationship to the Extension 2 Zone E1E ore zone and the Webb Lake Stock. Redrawn after a cross-section from Island Gold mine.

3.3 Structural Geology of the Study Area

A minimum of three generations of deformation were identified in the study area on the basis of overprinting relationships. They were documented through field mapping, detailed outcrop mapping, and structural measurements.

3.3.1 D1: Regional compression

D1 structures consist of regional F1 folds and the associated axial planar cleavage S1. F1 folds are upright, regional- and camp-scale folds. The Goudreau Anticline (Figure 2.4) is an example of such a regional F1 fold, the closure of which is located approximately 2 km southeast of the study area. The volcanic packages within the study area are located on the northern limb of the Goudreau Anticline and are tilted to their current, steeply NNW-dipping orientation as a result of F1 folding. A parasitic, camp-scale synclinal F1 fold within the study area (the "Magino fold") can be traced on surface by the S-pattern of the Michipicoten Iron Formation to the west of Goudreau Lake (Figure 3.1), and in drill core by the repetition of the contact between the Catfish and Wawa assemblages. The Webb Lake Stock occurs coincident to the axial plane of the Magino fold and obscures the fold nose, however the surface pattern and drill intersections suggest that the fold hinge plunges shallowly to moderately toward the west.

An S1 cleavage is developed axial-planar to F1 folds but is rarely preserved in the study area. The orientations of D1 and D2 structures are broadly coincident within the study area, and consequently S1 cleavage is pervasively overprinted and rarely recognizable as a distinct fabric. It is best preserved along the margins of intrusions, where it has often been rotated to a shallowly-dipping to sub-horizontal orientation.

Southeast of Goudreau Lake, pencil cleavage resulting from the intersection of sub-horizontal S1 and sub-vertical S2 fabrics is exposed along a historic logging trail to the south of Goudreau Lake. At the historic Portage Showing between Bearpaw Lake and Pine Lake, S1 cleavage can be traced in an intermediate intrusion surrounding folded lapilli tuff.

The orientation of upright, large-scale F1 folds indicates that D1 deformation took place during regional, roughly N-S compression. During D1 deformation, the Webb Lake Stock was intruded along the axial plane of a parasitic F1 fold. The elongate geometry of the stock and its coincidence with the fold axial plane suggests that deformation was ongoing during the time of emplacement. A contemporaneous intrusion, the trondhjemitic Gutcher Lake Stock (Turek et al.,1984; this study), is located in the western domain of the Goudreau Lake Deformation Zone. It displays an aureole of epidote-hornblende hornfels contact metamorphism that has been overprinted by regional greenschist-grade metamorphism (Studemeister, 1983), indicating that emplacement of the Gutcher Lake Stock, and by association, the Webb Lake Stock and D1 deformation, occurred before regional greenschist-grade metamorphism.

3.3.2 D2: Sinistral, north-side-up transpression

The Goudreau Lake Deformation Zone and associated penetrative S2 foliation, L2a stretching lineation, and L2b ductile slickenside striation were developed during D2 deformation and regional greenschist-facies metamorphism.

The Goudreau Lake Deformation Zone is a regional structure associated with gold mineralization. It has a gently sigmoidal trend, striking 090° in the western domain, 070° in the northern and southern domains, and 090° in the eastern domain

(Arias & Heather, 1987). In the northern and southern domains, where the study area is located, the deformation zone is centred on the contact between two volcanic assemblages (Figure 2.4).

S2 foliation is a pervasive, penetrative foliation that formed sub-parallel to the strike of the Goudreau Lake Deformation Zone. It is defined by flattened and elongated quartz–feldspar phenocrysts and lapilli and aligned micaceous minerals (Figure 3.6b) and has a preferred NE-SW strike in the study area. Within the study area, strikes range from 040° to 085° with a range in dips from sub-horizontal to sub-vertical (Figure 3.7; Figure 3.8). At the Morrison No.1 iron range (Figure 3.1), steeply south-dipping S2 foliation is observed to intersect the steeply north-dipping tuff-iron formation contact at an acute angle (Figure 3.6a). South of Goudreau Lake a D2 C-S fabric displaying sinistral shear sense is observed in intermediate tuff. At the historic Portage Showing, pre-D2 rusty millimetre-wide quartz veins are observed to be folded and offset along S2 foliation with north-side-up movement (Figure 3.6c). North of the past-producing Magino mine, sinistrally "stacked" flattened quartz–feldspar phenocrysts are present along the S2 foliation in tuff (Figure 3.6b). Within the Webb Lake Stock, S2 foliation occurs in sporadic bands and is best developed along contacts with xenoliths and external metavolcanic units. When plotted on a stereonet, the poles to S2 foliation form a girdle (Figure 3.10). The pole to this girdle is coincident with F3 fold axes, indicating that the wide range in the orientation of S2 foliation is due to overprinting by D3 deformation. Based on the small angle to S0 and the orientation of S2 fabric within areas where it is relatively well-preserved, the original orientation of S2 foliation is interpreted to be 070°-075° in strike with a sub-vertical dip. D3 deformation

subsequently rotated much of the foliation to an either steeply north- or south-dipping foliation and produced shallowly- to steeply-dipping fold limbs. The development of a steep foliation at a sub-parallel to oblique angle to the central domain of Goudreau Lake Deformation Zone is consistent with the transpressional characteristics laid out by Fossen et al. (1994).

The stretching lineations L2a are developed on penetrative S2 foliation within dacitic tuff and is defined by stretched quartz-feldspar phenocrysts (Figure 3.6c). They plunge moderately to the east to sub-vertically. L2a lineations are observed on sub-vertical to steeply dipping outcrop faces that are coincident with S2 foliation throughout the study area. When plotted together, their orientations fall on a continuum, varying from moderately southeast plunging to sub-vertical (Figure 3.8). The pattern of progressively steeper stretching lineations is consistent with those found in a transpressional regime (Lin et al., 1998), and the counter-clockwise progression is indicative of sinistral shear sense.

Ductile slickenside striations L2b are developed in micaceous minerals on S2 foliation surfaces in high strain areas and are sub-horizontal. Chlorite and sericite slickenfibres step counter-clockwise, indicating a sinistral sense of movement. The presence of sub-horizontal L2b lineations suggests that the simple shear component of deformation was concentrated in discrete zones, such as the high strain zones to the north and south of the Webb Lake Stock. The co-existence of both sub-horizontal and sub-vertical lineations is further evidence that deformation took place within a transpressional regime (e.g. Tikoff & Greene, 1996; Lin et al., 1998).

The formation of the sinistral Goudreau Lake Deformation Zone and associated structures during D2 deformation indicate that deformation took place within a north-side-up, transpressional regime. Chlorite and sericite are intimately associated with D2 structures and therefore metamorphism during D2 deformation is estimated to be greenschist facies. Further work on the metamorphism and alteration associated with the Island Gold deposit was conducted by T. Ciufo (2019).

3.3.3 D3: Dextral, south-side-up transpression

Structures related to D3 deformation pervasively overprint D1 and D2 structures within the study area. They consist of camp- and outcrop-scale F3 folds, associated S3 axial planar cleavage, and top-to-NW thrust faults.

F3 folds are open-to-tight, shallowly-plunging to sub-horizontal Z-folds. They occur at the outcrop scale where they transpose S2 foliation and deform small dykes, and at the camp and mine scale where they deform lithologic boundaries and the shape of the ore body. To the north of Goudreau Lake, in the northeast corner of the study area, a camp-scale F3 fold can be traced in the boundary between Cycle 2 intermediate tuff and Cycle 3 mafic metavolcanics (Figure 3.1). The Michipicoten Iron Formation, which occurs at this contact, is folded into a kilometer-scale Z-fold with a long limb trending 240° and short limb trending 230°. Mine-scale F3 folds deform the Main Island and Island Extension ore zones. The average orientation of the ore zones is 070°/80°S, but recorded dips range from 80°N to 75°S. In the cross-sections, the ore zones are observed to be deformed into a mine-scale, open F3 fold with long limbs dipping sub-vertically and the short limb dipping 75°S. Outcrop-scale F3 folds are developed proximal to felsic intrusions. They are particularly well developed within

chlorite schist but are observed in multiple lithologies. Immediately west of the historic Cabin Showing a lens of chlorite schist within the Webb Lake Stock displays intense F3 folding (Figure 3.12). S1 foliation and small quartz veins are transposed into decimeter-scale, shallowly west-plunging F3 Z-folds. The folds are asymmetric with an average orientation of long limbs at 250°/75°N, short limbs at 230°/25°N, and fold hinges plunging 07° toward 249°.

Within the mafic metavolcanic rocks east of the Morrison No.1 fold, an F3 z-fold is developed in proximity to a thin (<1 m) felsic dyke that has also been folded (Figure 3.10). A S2 foliation within the mafic metavolcanics is folded into a decimeter-scale F3 fold which plunges shallowly to the southwest (Figure 3.10c). The felsic dyke is located 3 meters to the north within the same outcrop and trends 235°. In the sub-vertical western edge of the outcrop, the felsic dyke is folded into an open, meter-scale F3 fold which rolls from 235°/75°N, to sub-horizontal, to 055°/65°S before the face is buried (Figure 3.10a). F3 folds are less developed within intermediate tuff and commonly occur as gentle, open folds. At the historic Portage Showing between Bearpaw Lake and Pine Lake, outcrop-scale F3 folds are observed in a historic trench (Figure 3.11) and in the walls of a historic pit. In the trench, an open meter-scale F3 fold with minor parasitic folds is developed in intermediate lapilli-tuff immediately south of a felsic intrusion. S2 foliation within the tuff is folded into gentle rolls and displays a continuum from sub-vertical, to south-dipping, to shallowly north-dipping, before the southern edge of the trench drops off sub-vertically (Figure 3.11c). These folded foliations describe a sub-horizontal to shallowly east-plunging fold hinge. The western edge of the trench is cut by a 325°-trending, relatively recessive diabase dyke which exposes a sub-vertical face of

the tuff roughly perpendicular to foliation. Here, the folded foliation is observed dipping steeply north in addition to the previously described range. Within the felsic intrusion occupying the northern area of the trench, a lens of chlorite schist is strongly deformed with folded S2 foliation at 245°/60°N and displays decimeter scale F3 folding. S2 foliation within the felsic intrusion has been rotated to 240°/75°N. The historic pit is located in intermediate tuff approximately 30 meters east-southeast from the trench. In the east and west walls of the pit S2 foliation is transposed into a gently curved, open F3 fold. The two visible limbs are oriented at 240°/55°N and 065°/75°S with a fold hinge plunging 05° toward 245°. The relative preservation of S2 fabric orientation proximal to intrusions implies that the extent of F3 folding is mitigated by the presence of a more competent body.

Steeply north-dipping S3 axial planar cleavage overprints S2 foliation and is weakly to moderately developed within felsic intrusions that have been affected by F2 folding (Figure 3.10b). North of Goudreau Lake, the majority of S2 foliation has been transposed to steeply north-dipping and sub-parallel to S3 axial planar cleavage.

Top-to-NW reverse faults that offset the ore zone underground were developed late during D3, likely as a result of strain accumulation.

Due to the steep S3 axial planar cleavage and the dextral z-form of F3 folds, D3 deformation is interpreted to have taken place during south-side-up transpression.

3.3.4 Late, undifferentiated deformation

Late deformation consists of pervasive crenulation cleavage, brittle fractures which show varying degrees of offset, and the emplacement of northwest-trending diabase dykes.

Lineation L4+ is a sub-horizontal to north-plunging crenulation cleavage that locally and pervasively overprints all previous structures throughout the study area. It is visible at both outcrop and thin-section scale. Within the historic trench at the Portage showing, millimetre-scale, moderately north-plunging crenulation cleavage L4+ offsets S2 foliation with top-to-north movement.

Late, brittle fractures are typically sub-vertical and produce minor (<1m) offset where markers, such as contacts, are present (Figure 3.11a).

Matachewan diabase dykes occur throughout the study area and may be associated with a portion of the late brittle fractures. Dykes are typically metre to decametre scale with a northwest strike and sub-vertical dip. In the Island Gold deposit, two diabase dykes separate the Extension 1 and Extension 2 zones from the main Island and Island Deep zones (Figure 3.1). The offset of the zones across the dykes suggests that the Matachewan dykes may have been emplaced along brittle faults.

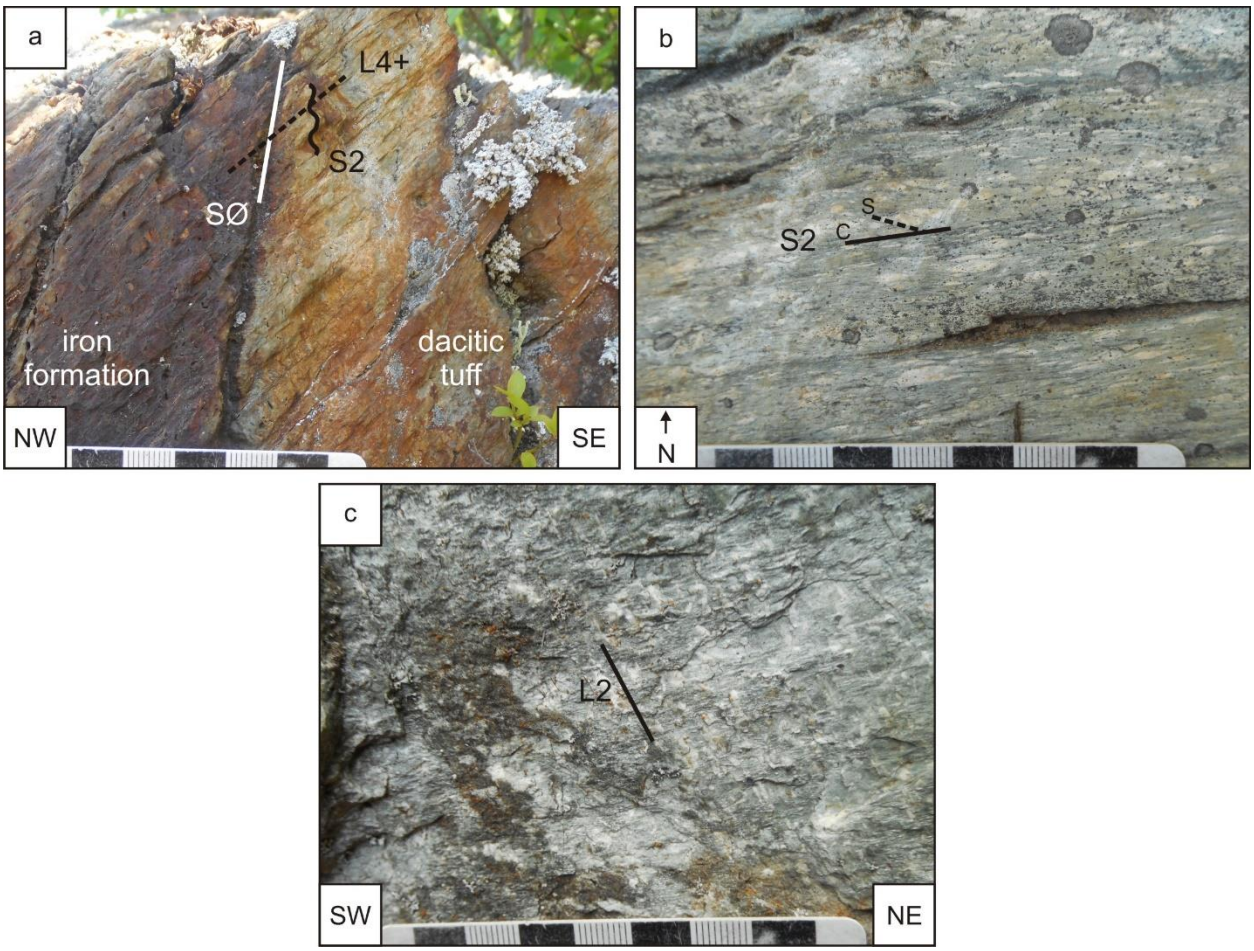

Figure 3.6: Outcrop photographs of D2 deformation structures found in the study area. a) Vertical outcrop surface showing south-dipping S2 foliation at a small angle to the north-dipping contact between Wawa assemblage dacitic tuff and the Morrison No.1 Iron Range (Michipicoten Iron Formation). S2 foliation is overprinted by north-plunging L4+ crenulation lineation. b) Horizontal outcrop surface displaying sinistral S2 foliation in dacitic phenoclastic tuff. c) Vertical outcrop surface displaying northeast-plunging L2 stretching lineation.

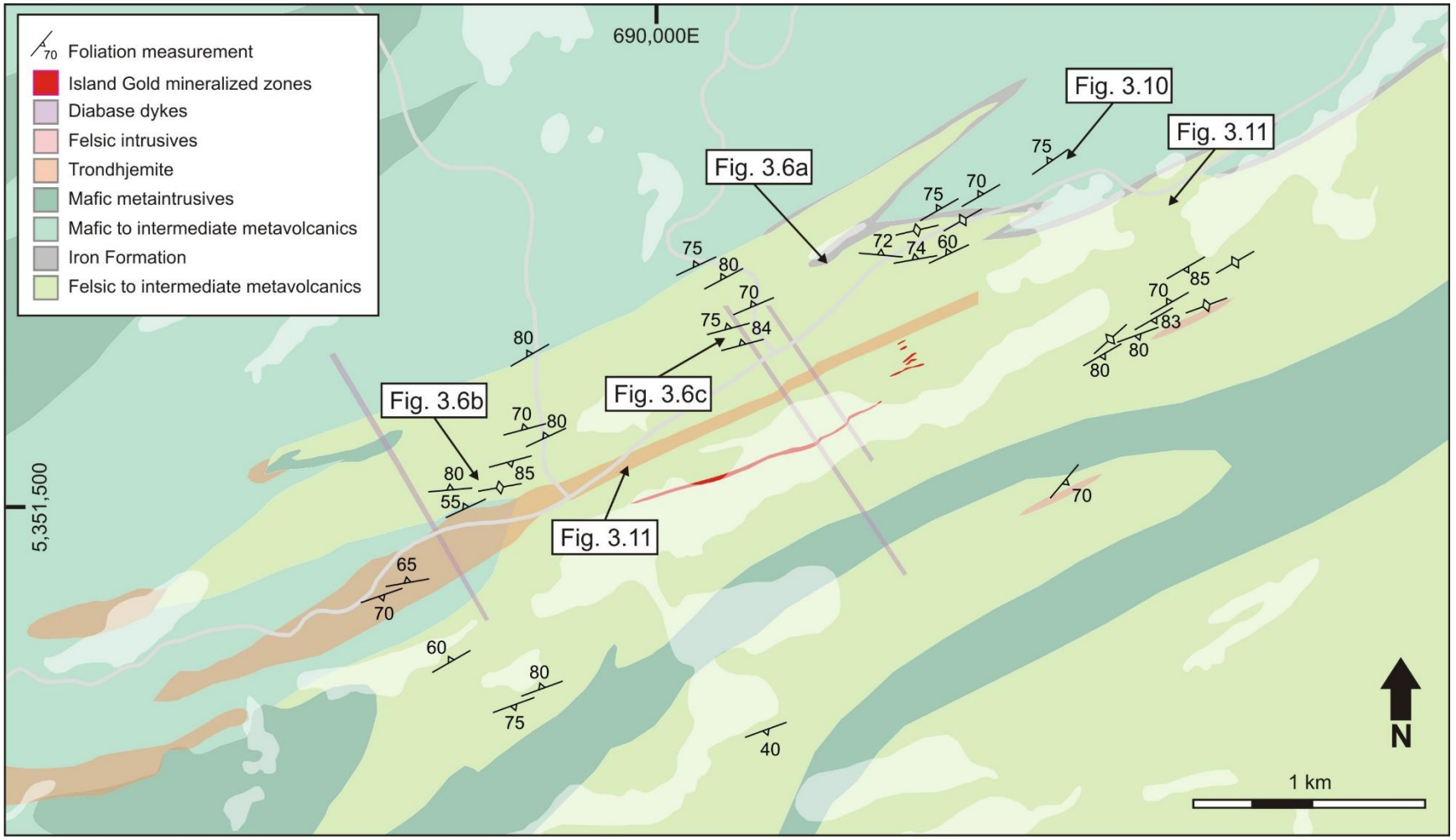

Figure 3.7: Foliation strike and dip measurements taken during the course of this study shown on a simplified geological map. Base map modified from mapping done by the mine geologists at Island Gold and Magino mines.

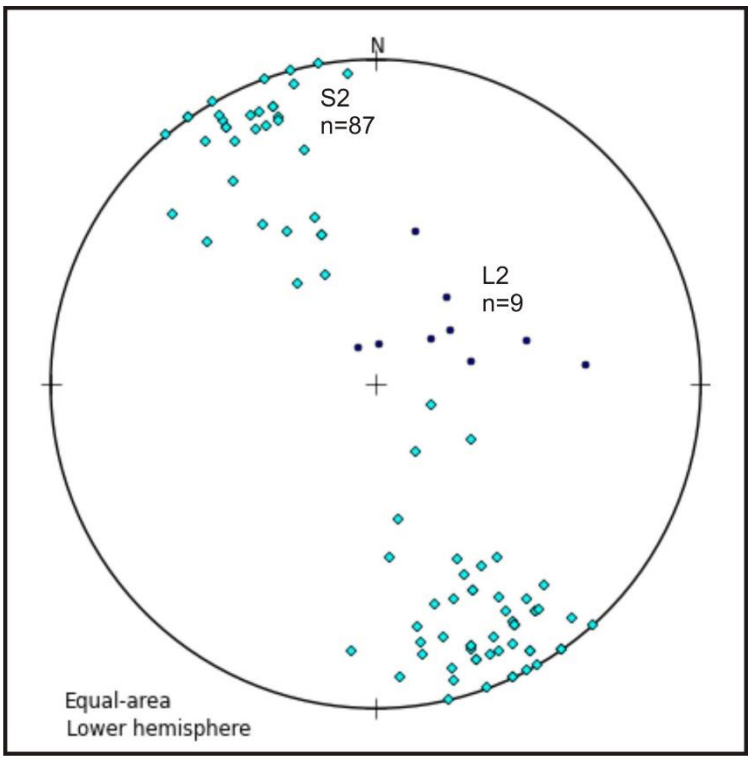

Figure 3.8: Lower hemisphere equal area plot showing the orientations of D2 fabrics in the study area. Light blue diamonds represent poles to S2 foliation planes. Dark blue dots represent L2 stretching lineations.

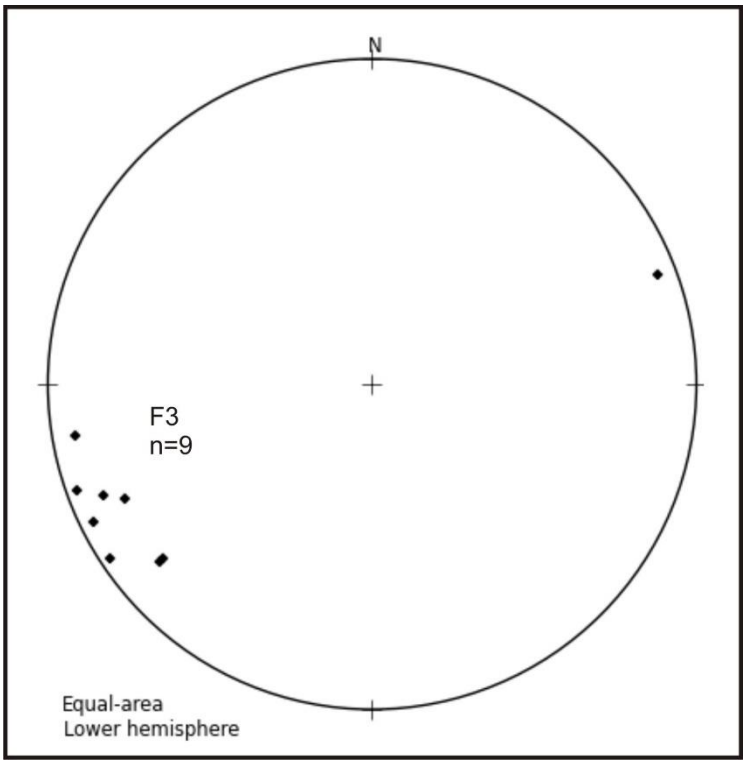

Figure 3.9: Lower hemisphere equal area plot showing the orientations of D3 folds in the study area. Black diamonds represent F3 fold hinges.

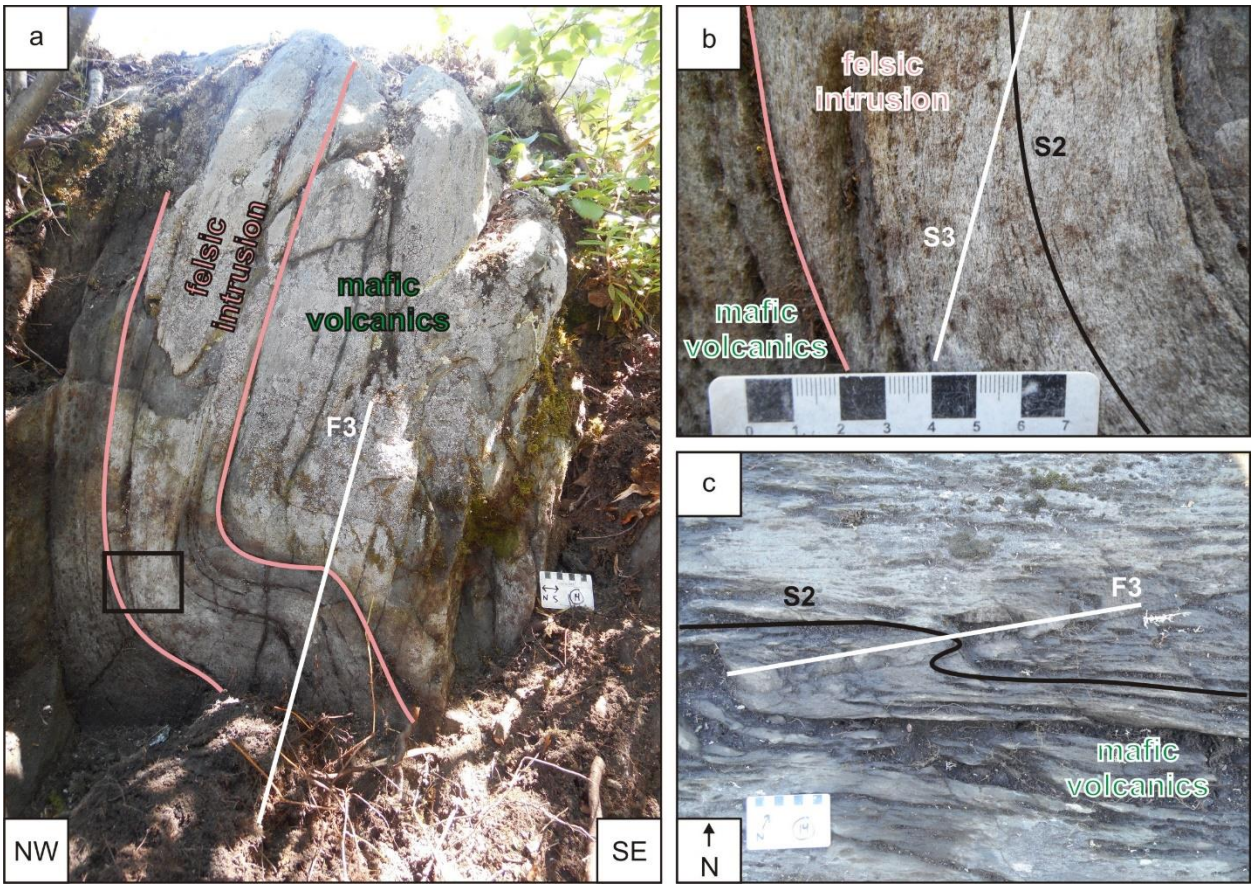

Figure 3.10: Outcrop photographs showing D3 folding of S2 foliation, preserved by the presence of a felsic intrusion. a) Vertical outcrop surface showing F3 folding of a felsic intrusion in mafic volcanics of the Catfish assemblage. b) Detail from (a) showing S2 foliation folded and overprinted by S3 axial-planar cleavage. c) Horizontal outcrop surface proximal to (a) showing S2 foliation in mafic volcanics overprinted by F3 folding.

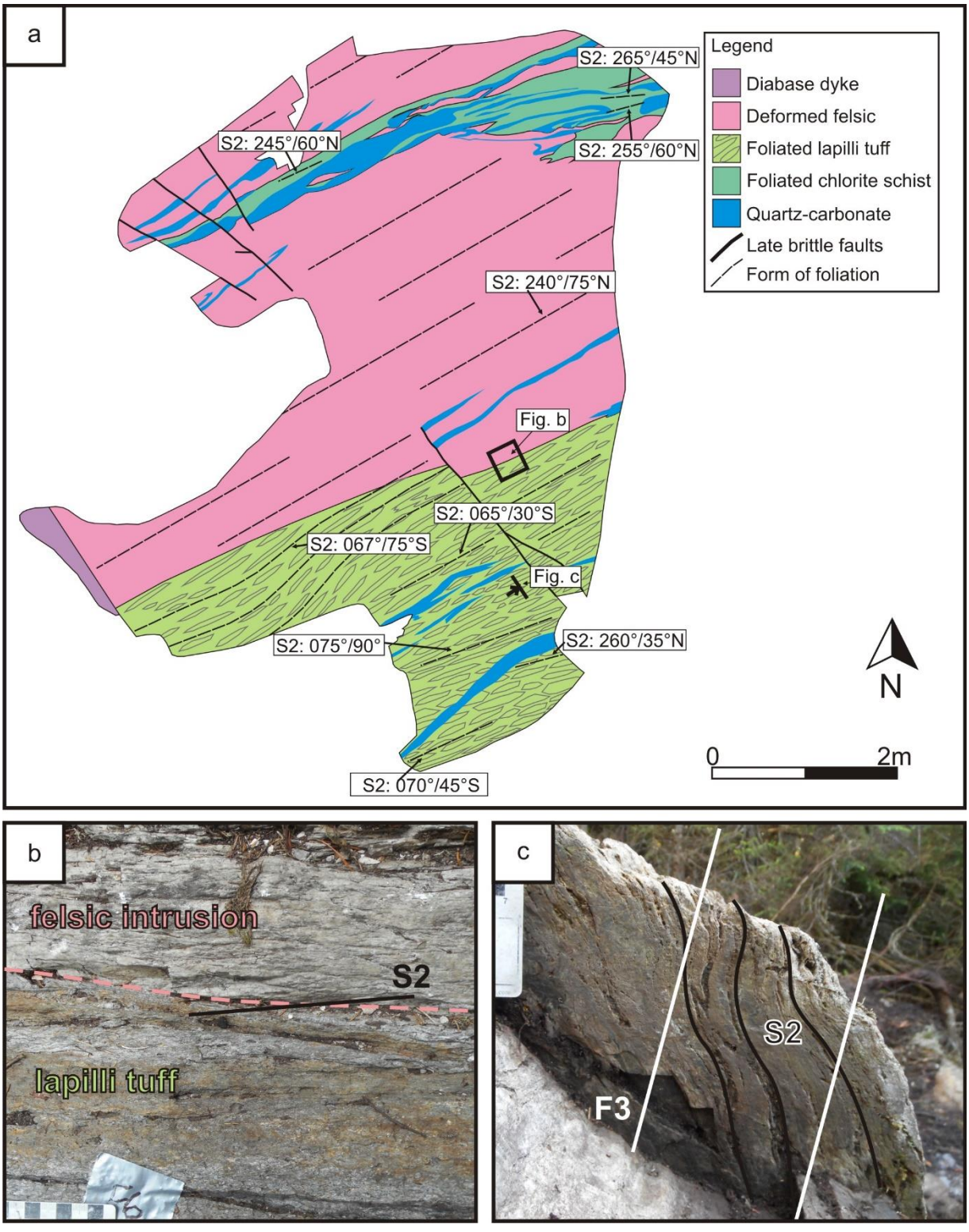

Figure 3.11: Detailed map of an outcrop immediately north of Pine Lake, showing fabrics related to D2 and D3 deformation, and highlighting the preservation of D2 fabrics proximal to intrusive bodies. a) Detailed outcrop map. b) Close-up of photograph of the contact between the Wawa assemblage lapilli tuff and a felsic intrusion showing the continuation of S2 foliation across the contact. c) Photograph of vertical surface showing S2 foliation gently folded along F3 fold axes.

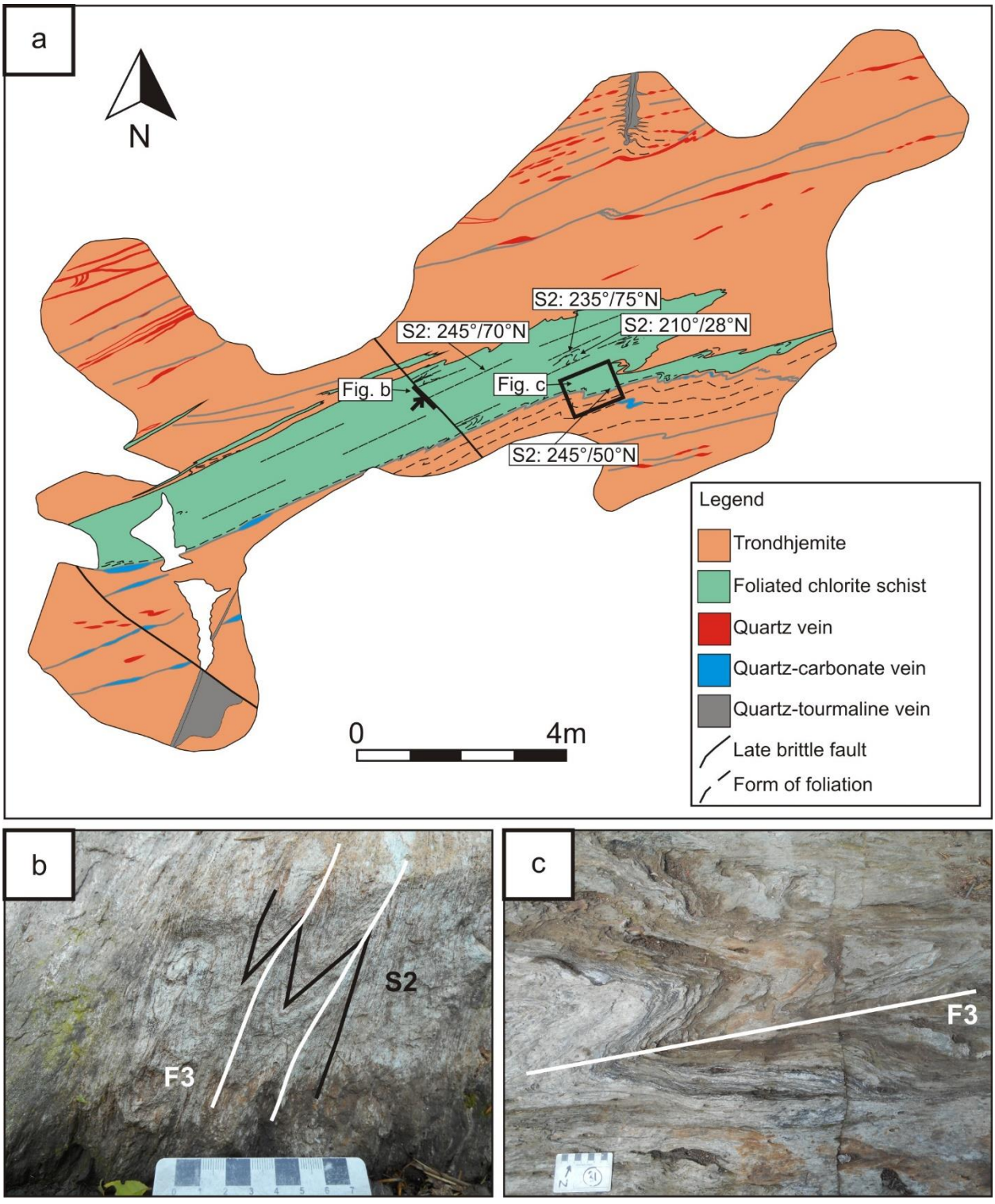

Figure 3.12: Detailed map of an outcrop immediately north of Goudreau Lake within the Webb Lake Stock, showing fabrics related to D2 and D3 deformation. a) Detailed outcrop map. b) Photograph of vertical outcrop surface showing S2 foliation in chlorite-schist tightly folded along F3 fold axes. c) Photograph of horizontal outcrop surface showing tight folding of the contact between chlorite-schist and the Webb Lake Stock along a shallowly west-plunging F3 fold hinge.

4. Vein Sets and Associated Mineralization of the Study Area

4.1 Introduction

Gold mineralization at the Island Gold mine is primarily hosted by quartz veins, with only minor mineralization present in wall rock proximal to veins. Through detailed underground and surficial investigation and mapping, five generations of veins have been identified (V_{GD}, V1, V2, V3, and V4).

4.2 Vein Sets

4.2.1 V_{GD}

V_{GD} veins occur almost exclusively in the Goudreau Zone of the Island Gold deposit. Due to the spatial separation between the Goudreau Zone and the main Island Zones, direct relative timing relationships between the two have not been established and therefore the V_{GD} veins have received a designation separate from the numbered vein sets. V_{GD} veins are mineralized, sub-horizontal extensional quartz-carbonate veins with minor sericite and often contain tourmaline cores. Vein thickness varies from 1 cm to 40 cm, typically decreasing where the vein has been sheared and reaching maximum thickness in fold noses. They have been folded into tight upright folds with shallowly east-plunging fold hinges (Figure 4.2). Primary extensional features, such as bridging structures, are often preserved within the veins (Figure 4.3a). Gold mineralization within V_{GD} veins can be very high grade (>1000 g/t in some chip samples), but it is typically discontinuous and nuggety. Visible gold is common and is most often observed as aggregates within the quartz. V_{GD} veins are hosted by the Webb Lake Stock, dioritic intrusions, and felsic to intermediate metavolcanics of the upper Wawa assemblage.

4.2.2 V1

V1 veins are dominant veins of the Island Gold deposit. They contain high-grade concentrations of gold, and most are steeply south-dipping laminated quartz shear veins with minor sericite, chlorite, and pyrite that strike sub-parallel to ore zone boundaries. They also occur as sub-horizontal buckled extensional veins. The majority of mineralization within the Island Gold deposit is hosted by V1 veins and visible gold is commonly observed as aggregates and disseminated grains in the quartz and as grains along chlorite-sericite slickensides within the veins (Figure 4.3c). V1 veins are hosted by dacitic metavolcanics and are enveloped by the "API" sericitic-silicic alteration package. The laminated veins occur as sub-parallel elongated lenses of smoky-grey to milky-white laminated quartz veins, typically 10 to 40cm thick and spaced 1 to 3 metres apart within ore zones. The lamination is defined by layers of quartz shear veins and slivers of highly sericitic-silicic-chloritic altered, foliated wall rock. Internal folding is common, and veins are extensively deformed and recrystallized with local brecciation. The sub-horizontal veins are composed of mostly massive smoky-grey to milky-white quartz with wall rock and sericite-chlorite-pyrite inclusions.

Petrographic study reveals that V1 veins are nearly entirely composed of quartz with accessory (<5%) sericite, chlorite, and pyrite. Quartz grains are subhedral with straight grain boundaries and sub-grains are common while undulose extinction is rare. Slickensides within the veins are predominantly sericite with variable amounts of chlorite and pyrite and show a reduced grainsize in quartz.

Within the Goudreau Zone, small laminated V1 veins are observed within weakly developed D2 shears. In the Island Zones, laminated V1 veins occur within D2 shearing,

sub-parallel to S2 foliation, suggesting they were likely emplaced during D2 deformation along dilated S2 c-surfaces. Sub-horizontal V1 veins occur at a high angle to laminated V1 veins and are buckled. The orientation of the sub-horizontal veins is compatible with the orientation of extension during D2 deformation and were therefore likely emplaced within extensional fractures during D2 deformation. Brittle D3 fractures containing V3 veins cross-cut V1 veins, indicating that V1 were emplaced prior to D3 deformation. Most V1 veins show brittle deformation (e.g. local brecciation), suggesting that they acted as a more competent body during later deformation. The margins of steeply-dipping V1 veins may have provided a preferred plane for movement during D3 deformation, resulting in the sharp southern contact of the C-zone mineralization.

4.2.3 V2

V2 veins are mineralized, discontinuous, millimetre- to centimetre-thick crack-seal veinlets spaced millimetres apart. They occur within the "API" alteration package, sub-parallel to laminated V1 veins and S2 foliation. Petrographic study shows that V2 veins are composed of fine-grained quartz, sericite, chlorite, and pyrite with minor gold. Within the ore zones, rock fabric has been destroyed by intense deformation and silicification, however the V2 veinlets appear to form along the orientation of D2 C-surfaces, suggesting that they were emplaced during D2 deformation and are likely broadly contemporaneous with V1 veins. V3 "boudin necks" deform the V2 veins into a pinch-and-swell fabric, indicating that V2 veins were emplaced prior to D3 deformation (Figure 4.3b).

4.2.4 V3

V3 veins are weakly mineralized extensional veins that cross-cut the Island Gold ore zones. They occur as shallowly-plunging and steeply-plunging boudin necks within V1 laminated veins, as shallowly-dipping extensional veins that cross-cut ore zones, and as en echelon veins along brittle thrust faults. In the main Island zones, sub-horizontal and sub-vertical V3 veins appear in N-S drift faces and in the "back" as elliptical boudin-necks within V1 veins (Figure 4.3b). In the Island Extension and Goudreau zones, shallowly south-dipping extensional V3 veins extend beyond the V1 veins into the surrounding alteration zone. Both the boudin-neck and extensional V3 veins commonly display sub-vertical growth fibres of quartz and carbonate. In the Island Extension Zone 1, V3 en echelon veins were locally associated with a south-dipping, top-to-northwest brittle thrust fault.

Petrographic study reveals that V3 veins are composed of varying amounts of quartz and carbonate. Both the quartz and carbonate components of V3 veins display a larger grainsize than that of V1 veins. Quartz grains within V3 veins display undulose extinction and sutured grain boundaries. V3 veins are weakly mineralized, but it is unclear whether the mineralization is primary or scavenged from the V1 veins that they cross-cut.

The orientation and opening direction of sub-horizontal and en echelon V3 veins are compatible with south-side-up transpression, suggesting that they were emplaced during D3 deformation. Where intersections between sub-horizontal and sub-vertical V3 veins are visible in drift walls, there is no apparent cross-cutting relationship,

indicating contemporaneous emplacement (Figure 4.3d). Blocky tourmaline is commonly found in V3 veins, but they are also cut by sub-vertical tourmaline “ribbons”.

4.2.5 V4

V4 veins are gold-barren tourmaline veins with minor quartz. The tourmaline occurs as ribbons, cores within other veins, and as blocky masses that invade or cross-cut all previous vein sets and fabrics. The prevalence of tourmaline decreases from west to east along the Main Island zones, becoming scarce within the Island Extension zones. V4 tourmaline ribbons follow, but also cross-cut laminated V1 veins. Within sub-horizontal V3 veins they commonly mimic the quartz-carbonate extensional growth fibres or form blocky masses. The I2M, an intrusion which cross-cuts the C-zone, commonly hosts sub-horizontal extensional quartz veins with V4 tourmaline cores. Petrographic study shows that tourmaline occurs as euhedral needles.

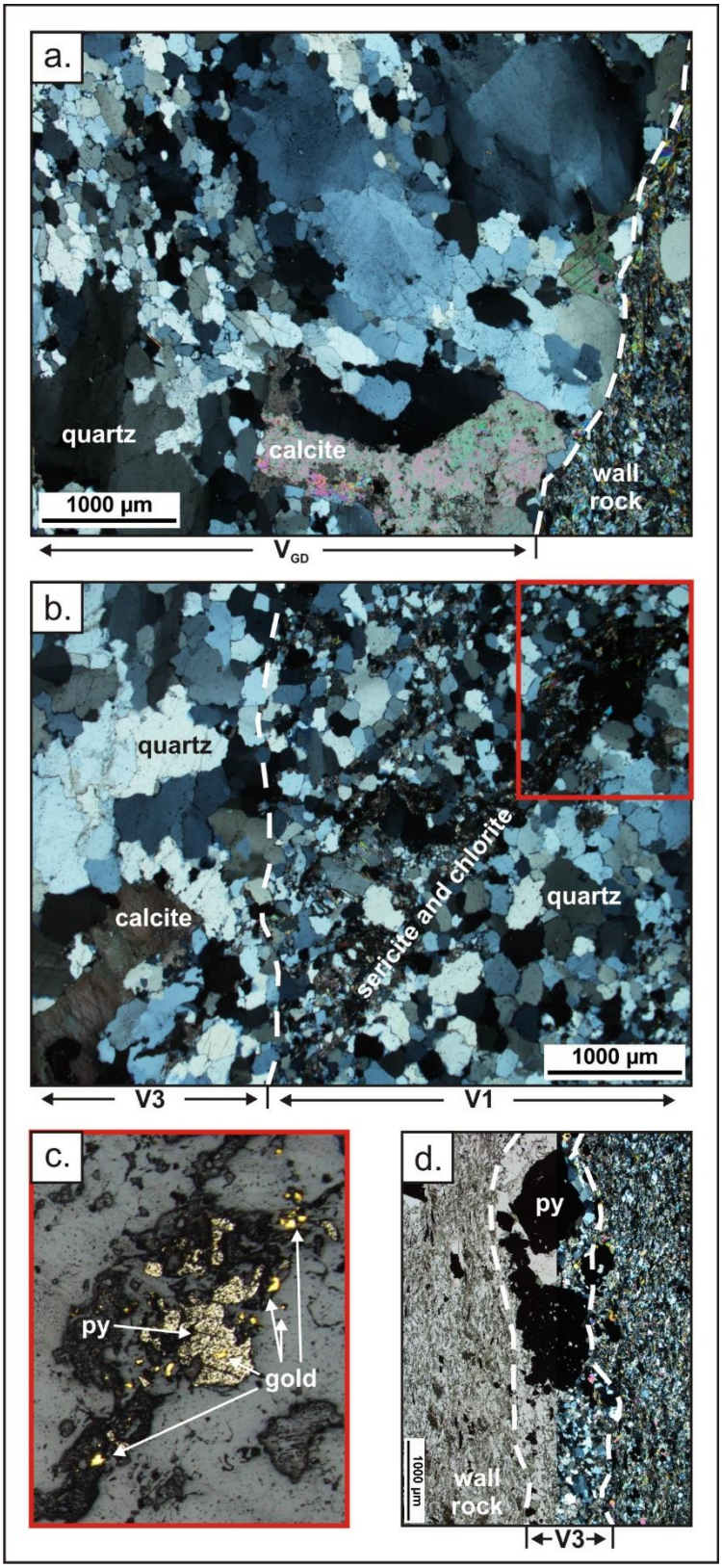

Figure 4.1: Thin section photomicrographs showing the petrography of main vein sets. a) V_{GD} vein with large quartz and calcite grains. Crossed nicols. b) V1 vein (right) cut by V3 vein (left). Crossed nicols. c) detail from (b) showing gold in pyrite and quartz. Reflected light. d) V2 vein in highly altered and crenulated wall rock. Plane polarized light (left) and crossed nicols (right).

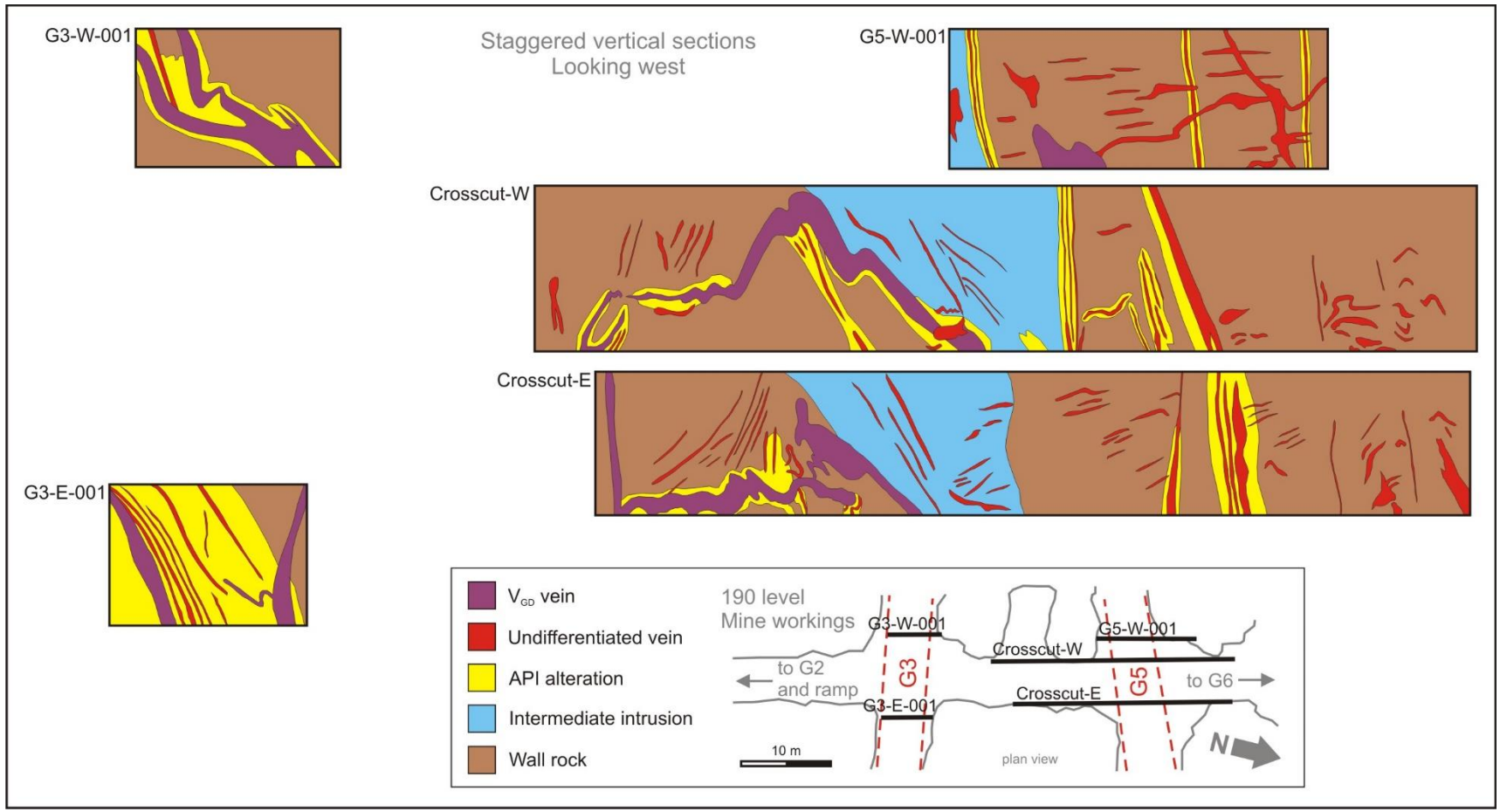

Figure 4.2: Diagram of V_{GD} veins on 190 level of Island Gold mine. Redrawn from diagram by H. Mellier at Island Gold with minor modifications.

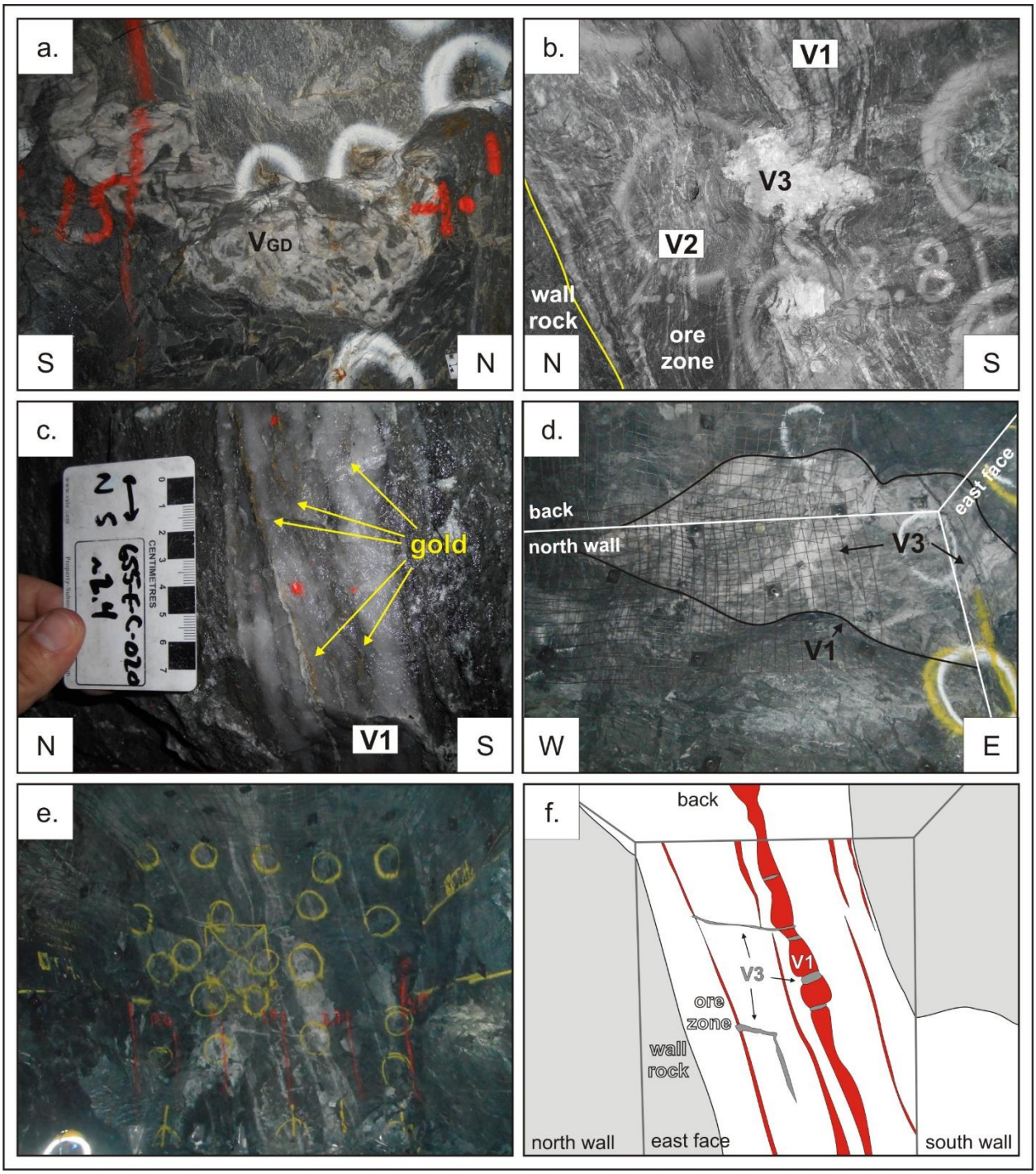

Figure 4.3: Photographs of vein sets found in the study area. a) V_{GD} vein in the Goudreau Zone. b) Cross-cutting relationship between V1, V2, and V3 veins in the main Island Zones. c) Visible gold occurring as suspended droplets and along slip faces in a V1 vein. d) The upper-left corner of a drift showing the orientation of a V3 conjugate vein set. e) A drift face in the Island Deep Zone showing the typical geometry of the C-zone: one of more steeply south-dipping, large V1 veins flanked by sub-parallel, smaller V1 veins and V2 veins within the ore zone and cross-cut by apparently sub-horizontal V3 veins. f) sketch of (e).

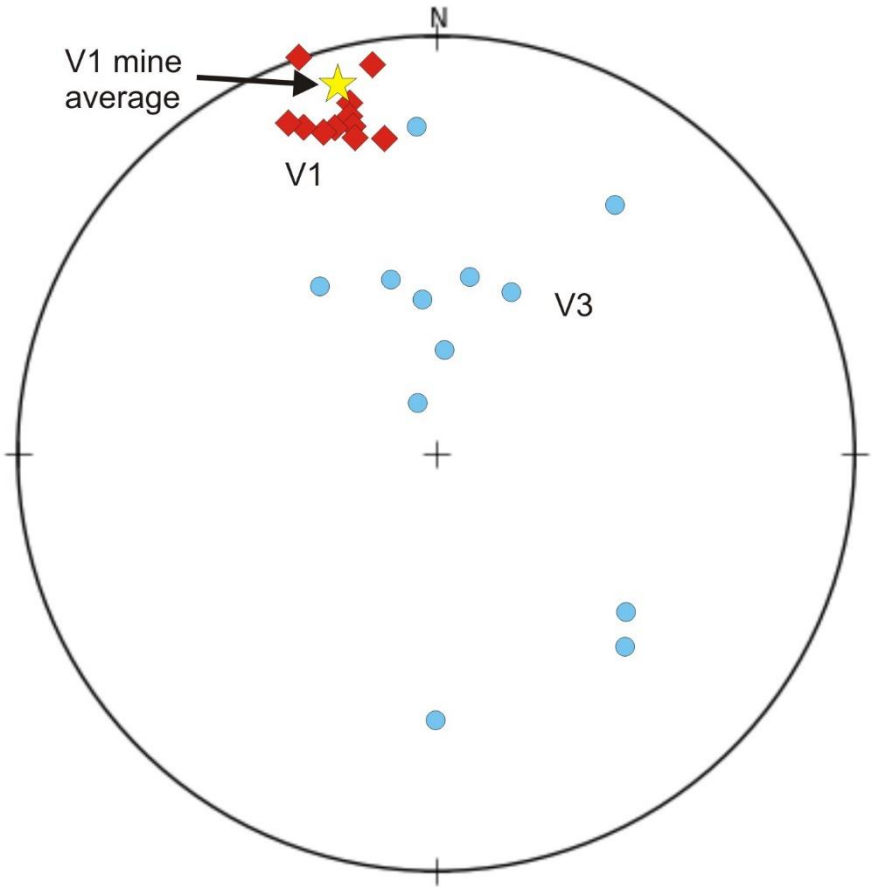

Figure 4.4: Lower hemisphere equal area projection showing the orientations of V1 and V2 veins sets in the Island Gold mine. Red diamonds represent poles to V1 veins recorded during this study. The yellow star represents the pole to the average orientation of Island Gold mine ore veins. Blue dots represent poles to V3 veins recorded during this study

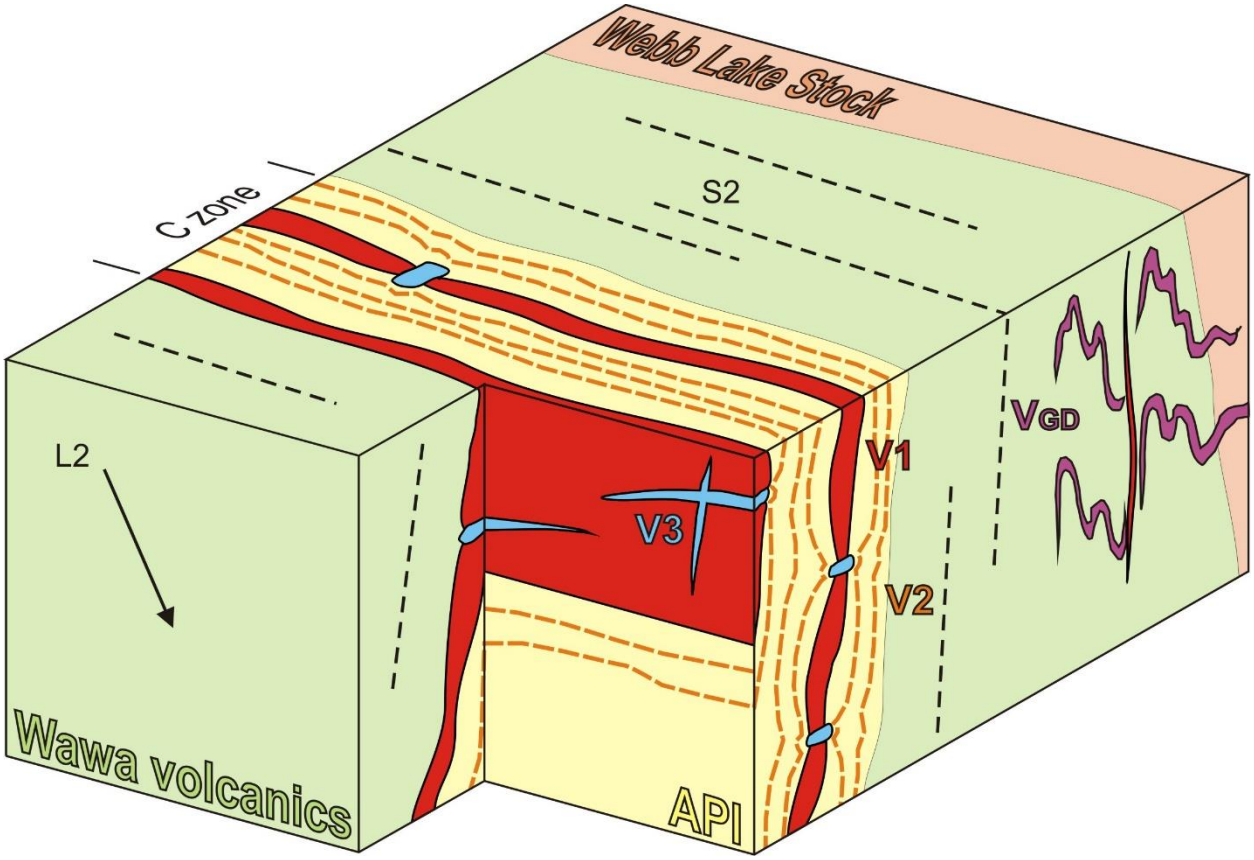

Figure 4.5: Schematic block diagram showing the geometry of D2 fabrics and the vein sets of the Island Gold deposit. API=Alteration Package Island. Not drawn to scale.

5. U-Pb Geochronology

5.1 Introduction

Two intrusions within the study area were selected for U-Pb geochronology to constrain the absolute age of gold mineralization at the Island Gold deposit. Samples were collected from core and underground and sent to the Geological Survey of Canada for processing and analysis.

5.2 Analytical Techniques

Zircons were separated from 1-5 kg of pulverised rock by conventional crushing, grinding, and hydrodynamic separation on a Wilfley™ table, Methylyne Iodine heavy liquid separation, and magnetic separation using a Frantz isodynamic separator. Zircons were selected from the magnetic and (or) non-magnetic fraction at 1.8 A and 1°ss. Around 70-130 grains from each sample were mounted in epoxy resin and polished to expose their interior.

U-Pb analyses were performed with the SHRIMP II instrument at the J.C. Roddick Ion Microprobe Laboratory, Geological Survey of Canada, Ottawa. Analytical procedures followed those described by Stern (1997). Briefly, zircons were cast in 2.5 cm diameter epoxy mounts along with fragments of the GSC laboratory standard zircon (z6266, with $^{206}Pb/^{238}U$ age = 559 Ma, Stern and Amelin, 2003). The mid-sections of the zircon grains were exposed using 9, 6, and 1 μm diamond compound, and the internal features of the zircon (such as zoning, structures, alteration, etc.) were characterized in back-scattered electron mode (BSE) utilizing a Zeiss Evo 50 scanning electron microscrope. Mount surfaces were evaporatively coated with 10 nm of high purity Au. Analyses were conducted using an $^{16}O^{2-}$ primary beam projected onto the zircon at 10 kV. The count rates at eleven masses including background were

sequentially measured over 6 scans with a single electron multiplier and a pulse counting system with deadtime of 23 ns. Off-line data processing was accomplished using SQUID version 2.50.11.10.15, rev. 15 Oct 2011. The 1σ external errors of $^{206}Pb/^{238}U$ ratios reported in the data table incorporate a minimum ±1.0 % error in calibrating the standard zircon (see Stern and Amelin, 2003). Pb isotopic values were monitored by analyses of an in-house standard with a $^{207}Pb/^{206}Pb$ age of 2679.6 ± 0.3 Ma; a small mass bias correction (1.003) was applied. Common Pb correction utilized the Pb composition of the surface blank (Stern, 1997). Isoplot v. 4.15 (Ludwig, 2008) was used to generate concordia plots and calculate weighted means. The error ellipses on the concordia diagrams and the weighted mean errors are reported at 2σ. Analytical data are given in tables 5.1 and 5.2.

5.3 Sample description and U-Pb results

5.3.1 Sample SH-3: Webb Lake Stock trondhjemite

Sample SH-3 is from the Webb Lake Stock, a mineralized trondhjemitic intrusion that extends sub-parallel to the Island Gold deposit, approximately 500 metres to the northwest. Sample material was collected from drill core which intersected the stock at 550 metres below surface. The elongate, stretched out shape of the stock suggests that it was emplaced syn-tectonically with the F1 fold that it intrudes along. Results from this sample will give an absolute older limit on the timing of mineralization and an approximate timing of D1 deformation associated with the emplacement of the Webb Lake Stock.

128 zircons were recovered from sample SH-3. The majority of zircons recovered were colourless, slightly elongate, sub- to euhedral crystals. Some of the zircons had a

brownish hue, and a few formed very long, slender crystals (Figure 5.2). SEM images of the zircons show zoned or faintly zoned grain interiors with homogenous rims or recrystallized zones (Figure 5.1). Twenty-four spot analyses were done on 22 zircons and; 4 were taken from rims and 20 were taken from the grain interior. Regardless of the location of the spot analysis, very similar ages were returned. Together, the analyses returned a weighted mean $^{207}Pb/^{206}Pb$ age of 2724.1±4.3 Ma (n=23/24; MSWD = 1.5) for sample SH-3. The precision of the age is indicative of a single age for the sample, and zoning is considered a product of magma crystallization. This places an older limit on the absolute timing of mineralization as well as an approximate time for D1 deformation.

5.3.4 Sample KJM095: "I2M" intrusion

Sample KJM095 is from the "I2M", a weakly deformed, barren, nepheline-bearing monzonite intrusion which cross-cuts the Island ore zones at depth and dips steeply to the north. Sample material was collected from the 740 level of the Island Gold mine workings. The absence of a pervasive fabric or alteration within the intrusion suggests that the I2M was emplaced late or after D2 shearing and regional greenschist-facies metamorphism. The results from this sample will give an absolute younger limit on the timing of mineralization, as well as the approximate timing of the end of D2 deformation.

Seventy zircons were recovered from sample KJM095. They were pale to dark translucent brown with subhedral to rounded crystals (Figure 5.4). SEM images of the zircons show zoned grain interiors with thin, homogenous rims (Figure 5.3). 24 spot analyses were done on 22 zircons; 3 were taken from rims and 21 were taken from the

grain interior. The ages returned for sample KJM095 were also remarkably similar regardless of spot location and define a weighted mean $^{207}Pb/^{206}Pb$ age of 2672.2±3.5 Ma (n=24/24; MSWD = 1.2). The data is indicative of a single age and represents the magma crystallization age. This places a younger limit on the absolute timing of mineralization as well as D2 deformation.

Table 1: U-Pb SHRIMP analytical data for sample SH-3 from the Webb Lake Stock.

Webb Lake trondhjemite SH-3; UTM Zone 16, 5352095.9N 690454.7E

Spot name	U (ppm)	Th (ppm)	Th/U	Yb (ppm)	Hf (ppm)	$^{204}Pb/^{206}Pb$	% ±	$f(206)^{204}$ %	$^{206}Pb^*$ (ppm)	$^{208*}Pb/^{206*}Pb$	±	$^{207*}Pb/^{235}U$	±	$^{206*}Pb/^{238}U$	±	Corr Coeff	$^{207*}Pb/^{206*}Pb$	±	Apparent Ages (Ma) $^{206}Pb/^{238}U$	±	Apparent Ages (Ma) $^{207}Pb/^{206}Pb$	±	Disc. (%)
12157-059.1	47	18	0.41	160	10344	5.9E-04	18	1.03	22.1	0.089	6.0	13.703	1.5	0.5500	1.2	0.798	0.1807	0.9	2825	28	2659	15	-8
12157-042.1	48	22	0.47	199	8616	1.7E-04	25	0.29	22.6	0.127	3.4	13.886	1.5	0.5456	1.2	0.795	0.1846	0.9	2807	27	2695	15	-5
12157-015.1	27	15	0.59	138	9066	2.2E-04	29	0.39	12.0	0.155	4.1	13.325	1.6	0.5221	1.3	0.855	0.1851	0.8	2708	30	2699	13	0
12157-013.1	58	25	0.45	221	8620	8.1E-05	33	0.14	25.3	0.121	3.0	13.100	1.2	0.5130	1.1	0.910	0.1852	0.5	2669	25	2700	8	1
12157-061.1	18	6	0.35	95	9942	1.7E-04	41	0.30	8.2	0.089	6.9	13.677	1.8	0.5353	1.5	0.844	0.1853	1.0	2764	35	2701	16	-3
12157-021.1	58	29	0.53	200	8337	8.1E-05	35	0.14	25.7	0.142	2.9	13.347	1.4	0.5185	1.2	0.812	0.1867	0.8	2693	25	2713	14	1
12157-001.1	81	35	0.45	191	10914	3.0E-05	45	0.05	36.6	0.124	2.4	13.537	1.1	0.5255	1.1	0.935	0.1868	0.4	2722	24	2715	7	0
12157-038.1	39	22	0.58	259	8151	5.9E-05	50	0.10	17.7	0.165	3.3	13.533	1.4	0.5244	1.3	0.888	0.1872	0.7	2718	28	2718	11	0
12157-026.1	52	25	0.50	200	8623	-1.1E-05	100	-0.02	24.1	0.135	3.0	13.867	1.3	0.5370	1.2	0.897	0.1873	0.6	2771	26	2719	10	-2
12157-061.2	100	57	0.59	249	11772	4.2E-05	35	0.07	46.3	0.160	3.1	13.873	1.1	0.5366	1.0	0.941	0.1875	0.4	2769	23	2720	6	-2
12157-009.1	74	38	0.53	259	9381	8.9E-05	28	0.15	33.2	0.145	2.4	13.579	1.2	0.5251	1.1	0.923	0.1875	0.5	2721	24	2721	7	0
12157-020.1	93	58	0.64	317	8161	-1.1E-05	71	-0.02	42.6	0.178	2.9	13.738	1.1	0.5309	1.0	0.941	0.1877	0.4	2745	23	2722	6	-1
12157-032.1	52	24	0.48	213	8680	9.6E-05	32	0.17	24.0	0.126	3.0	13.819	1.3	0.5339	1.2	0.908	0.1877	0.5	2758	26	2722	9	-2
12157-022.1	43	19	0.45	135	8804	7.2E-05	41	0.12	19.7	0.129	3.3	13.708	1.5	0.5287	1.2	0.806	0.1881	0.9	2736	27	2725	14	0
12157-006.1	67	38	0.59	230	9246	3.2E-05	50	0.06	29.8	0.154	2.4	13.453	3.0	0.5188	2.9	0.969	0.1881	0.7	2694	64	2725	12	1
12157-059.2	25	9	0.36	112	9691	2.5E-05	100	0.04	11.4	0.089	5.9	13.830	1.7	0.5331	1.5	0.867	0.1882	0.8	2754	33	2726	14	-1
12157-019.1	67	30	0.47	241	9178	3.7E-05	45	0.06	31.0	0.123	2.7	13.914	1.2	0.5356	1.1	0.926	0.1884	0.4	2765	25	2728	7	-2
12157-011.1	97	43	0.46	314	10421	6.6E-21	9999	0.00	42.9	0.128	2.1	13.419	1.1	0.5164	1.0	0.946	0.1884	0.4	2684	23	2729	6	2
12157-054.1	90	40	0.46	319	8901	-1.1E-05	71	-0.02	40.7	0.123	2.2	13.722	1.1	0.5276	1.0	0.941	0.1886	0.4	2731	23	2730	6	0
12157-035.1	59	26	0.47	243	8743	-2.0E-05	71	-0.03	26.3	0.125	3.1	13.603	1.3	0.5227	1.2	0.911	0.1887	0.5	2711	26	2731	9	1
12157-027.1	80	37	0.48	257	9488	2.4E-05	50	0.04	37.0	0.135	2.2	14.059	1.1	0.5401	1.1	0.937	0.1888	0.4	2784	24	2732	7	-2
12157-031.1	71	32	0.47	235	10305	-7.1E-06	100	-0.01	32.3	0.130	2.5	13.853	1.2	0.5319	1.1	0.932	0.1889	0.4	2749	24	2733	7	-1
12157-049.1	88	59	0.69	332	9078	2.9E-05	45	0.05	39.3	0.192	1.8	13.515	1.1	0.5178	1.1	0.938	0.1893	0.4	2690	23	2736	6	2
12157-023.1	57	24	0.43	244	9292	9.2E-05	32	0.16	25.8	0.117	3.1	13.829	1.3	0.5296	1.1	0.909	0.1894	0.5	2740	26	2737	9	0

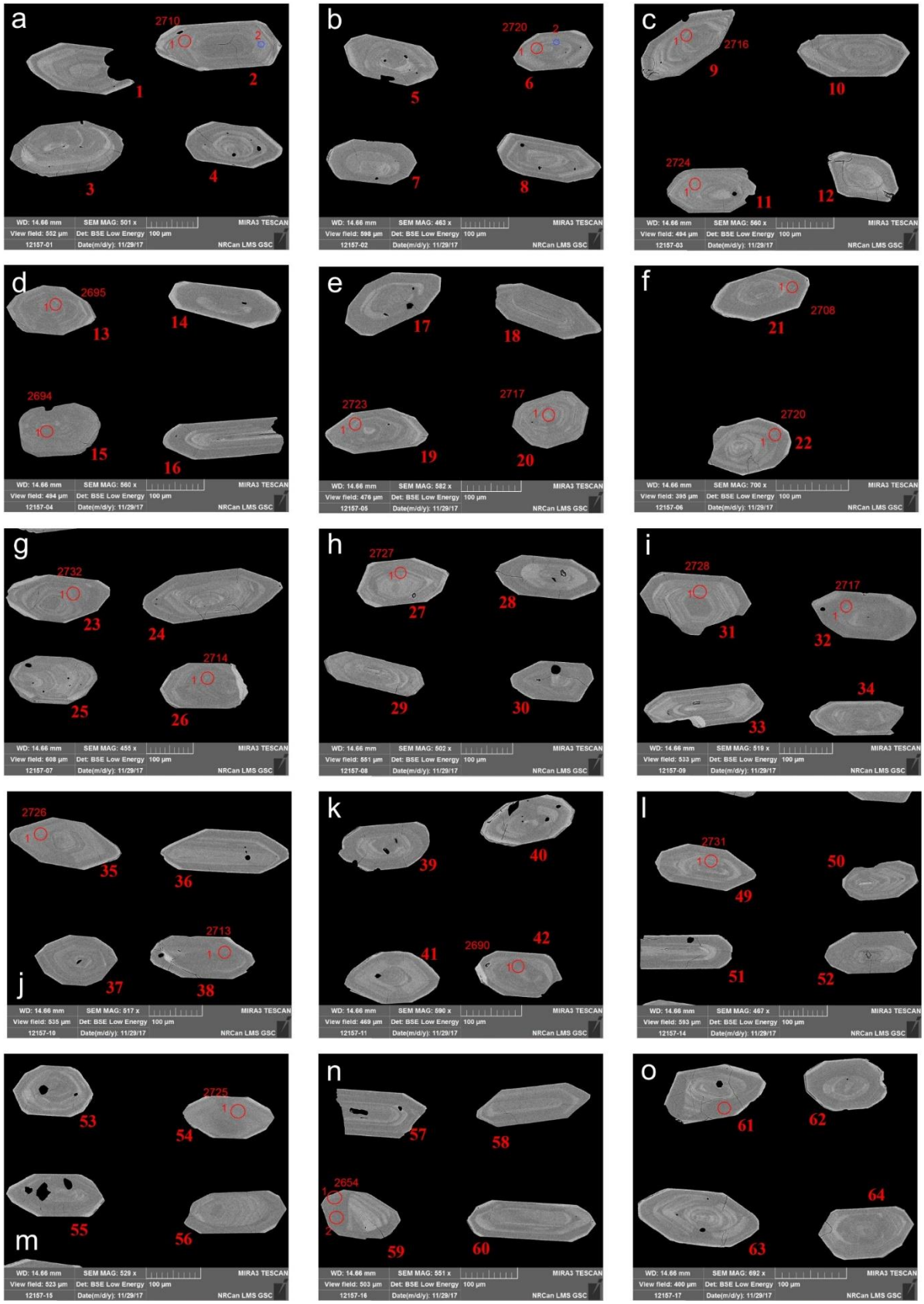

Figure 5.1: SEM BSE images of zircons analyzed from sample SH-3. Location of spot analyses indicated by red and blue circles with $^{207}Pb/^{206}Pb$ ages beside them.

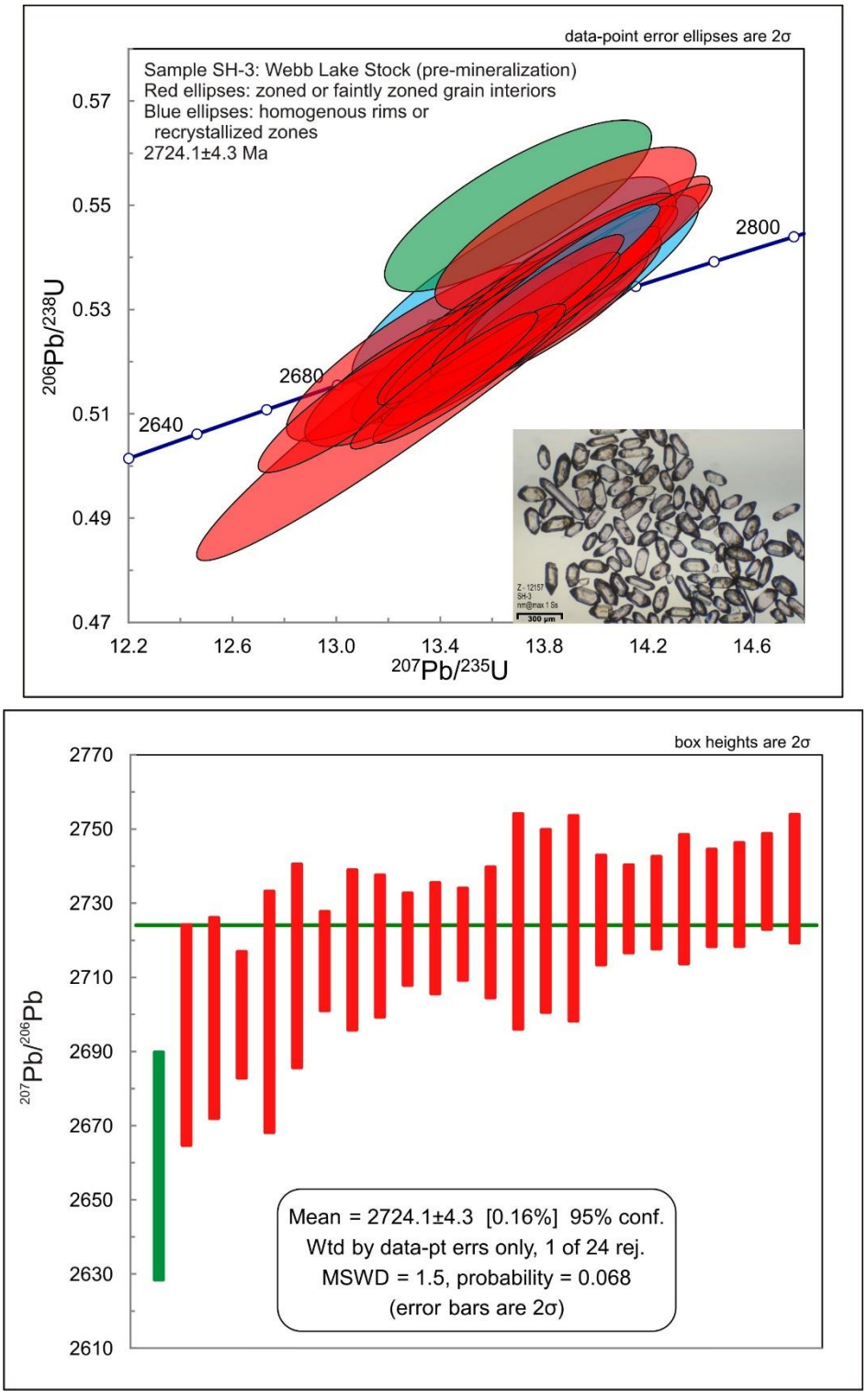

Figure 5.2: Concordia diagram and weighted average diagram showing data for sample SH-3 from the Webb Lake Stock. Excluded data point shown in green. Inset image shows zircon population after mineral separation.

Table 2: U-Pb SHRIMP analytical data for Sample KJM095 from the I2M intrusion.

Intermediate dyke KJM095; UTM Zone 16, 5351550.8N 690575.2E

Spot name	U (ppm)	Th (ppm)	Th/U	Yb (ppm)	Hf (ppm)	$^{204}Pb/^{206}Pb$	% ±	f(206)^{204} %	$^{206}Pb^*$ (ppm)	$^{208*}Pb/^{206*}Pb$	±	$^{207*}Pb/^{235}U$	±	$^{206*}Pb/^{238}U$	±	Corr Coeff	$^{207*}Pb/^{206*}Pb$	±	Apparent Ages (Ma) $^{206}Pb/^{238}U$	±	Apparent Ages (Ma) $^{207}Pb/^{206}Pb$	±	Disc. (%)
12156-041.1	408	117	0.30	211	9694	8.1E-06	45	0.01	181.3	0.081	1.5	12.892	1.0	0.5170	0.9	0.976	0.1808	0.2	2687	21	2661	3	-1
12156-036.1	371	161	0.45	255	7737	3.4E-05	50	0.06	164.1	0.131	2.7	12.884	1.2	0.5153	1.1	0.928	0.1813	0.4	2679	24	2665	7	-1
12156-059.1	580	351	0.63	181	8978	9.8E-07	100	0.00	247.8	0.171	0.8	12.449	1.0	0.4973	0.9	0.965	0.1816	0.3	2602	20	2667	4	3
12156-047.1	282	123	0.45	149	8544	5.9E-05	41	0.10	124.4	0.120	3.1	12.876	1.2	0.5140	1.1	0.921	0.1817	0.5	2674	24	2668	8	0
12156-028.1	507	247	0.50	232	8902	5.9E-06	45	0.01	224.0	0.140	1.5	12.882	0.9	0.5142	0.9	0.983	0.1817	0.2	2675	20	2668	3	0
12156-032.1	773	507	0.68	179	9180	6.2E-06	35	0.01	330.7	0.187	1.1	12.493	0.9	0.4983	0.9	0.988	0.1818	0.1	2606	20	2670	2	3
12156-001.2	400	189	0.49	275	8512	-1.3E-06	100	0.00	173.9	0.131	1.0	12.682	1.0	0.5057	0.9	0.981	0.1819	0.2	2638	20	2670	3	1
12156-045.1	471	313	0.69	299	9016	2.4E-06	71	0.00	206.8	0.190	0.8	12.824	0.9	0.5112	0.9	0.982	0.1820	0.2	2662	20	2671	3	0
12156-050.1	519	191	0.38	252	7881	7.8E-06	38	0.01	223.5	0.107	1.1	12.580	0.9	0.5013	0.9	0.983	0.1820	0.2	2619	20	2671	3	2
12156-015.1	470	207	0.45	258	9178	2.7E-06	71	0.00	199.7	0.123	1.1	12.413	1.0	0.4947	0.9	0.980	0.1820	0.2	2591	20	2671	3	4
12156-006.1	385	146	0.39	201	9543	-3.5E-06	71	-0.01	167.3	0.109	1.3	12.685	1.0	0.5054	0.9	0.975	0.1820	0.2	2637	20	2672	4	2
12156-033.1	586	372	0.66	337	9272	8.8E-06	35	0.02	256.7	0.182	0.8	12.802	0.9	0.5101	0.9	0.983	0.1820	0.2	2657	20	2672	3	1
12156-066.1	672	375	0.58	229	9903	2.1E-05	21	0.04	285.9	0.161	0.8	12.426	0.9	0.4950	0.9	0.985	0.1820	0.2	2592	20	2672	3	4
12156-018.1	653	239	0.38	276	8962	9.3E-07	100	0.00	281.7	0.104	1.0	12.610	0.9	0.5021	0.9	0.986	0.1821	0.2	2623	20	2673	3	2
12156-068.1	543	298	0.57	328	8904	-2.2E-06	71	0.00	234.8	0.155	0.9	12.643	0.9	0.5033	0.9	0.983	0.1822	0.2	2628	20	2673	3	2
12156-056.1	429	280	0.67	156	7724	7.7E-06	41	0.01	187.7	0.187	1.6	12.793	0.9	0.5092	0.9	0.981	0.1822	0.2	2653	20	2673	3	1
12156-041.2	278	116	0.43	218	8187	-7.7E-06	58	-0.01	124.4	0.118	1.6	13.096	1.0	0.5209	1.0	0.965	0.1823	0.3	2703	22	2674	4	-1
12156-044.1	669	424	0.65	194	9066	-2.7E-23	9999	0.00	283.7	0.180	0.8	12.407	1.3	0.4934	1.3	0.993	0.1824	0.2	2585	28	2675	3	4
12156-001.1	651	238	0.38	288	9943	5.3E-06	45	0.01	279.1	0.105	1.1	12.551	0.9	0.4991	0.9	0.984	0.1824	0.2	2610	20	2675	3	3
12156-046.1	687	437	0.66	187	9151	1.9E-06	71	0.00	300.2	0.183	0.8	12.787	0.9	0.5084	0.9	0.985	0.1824	0.2	2650	20	2675	3	1
12156-023.1	591	369	0.64	187	8796	2.1E-06	71	0.00	254.0	0.178	1.3	12.585	0.9	0.5001	0.9	0.984	0.1825	0.2	2614	20	2676	3	3
12156-064.1	553	290	0.54	211	9394	8.0E-06	38	0.01	237.4	0.151	0.9	12.576	0.9	0.4997	0.9	0.982	0.1825	0.2	2612	20	2676	3	3
12156-055.1	480	182	0.39	267	9941	2.2E-06	71	0.00	209.5	0.106	1.1	12.793	3.5	0.5083	3.4	0.981	0.1825	0.7	2649	74	2676	11	1
12156-053.1	604	377	0.64	180	8759	1.5E-05	26	0.03	254.0	0.178	0.8	12.318	0.9	0.4892	0.9	0.985	0.1826	0.2	2567	20	2677	3	5

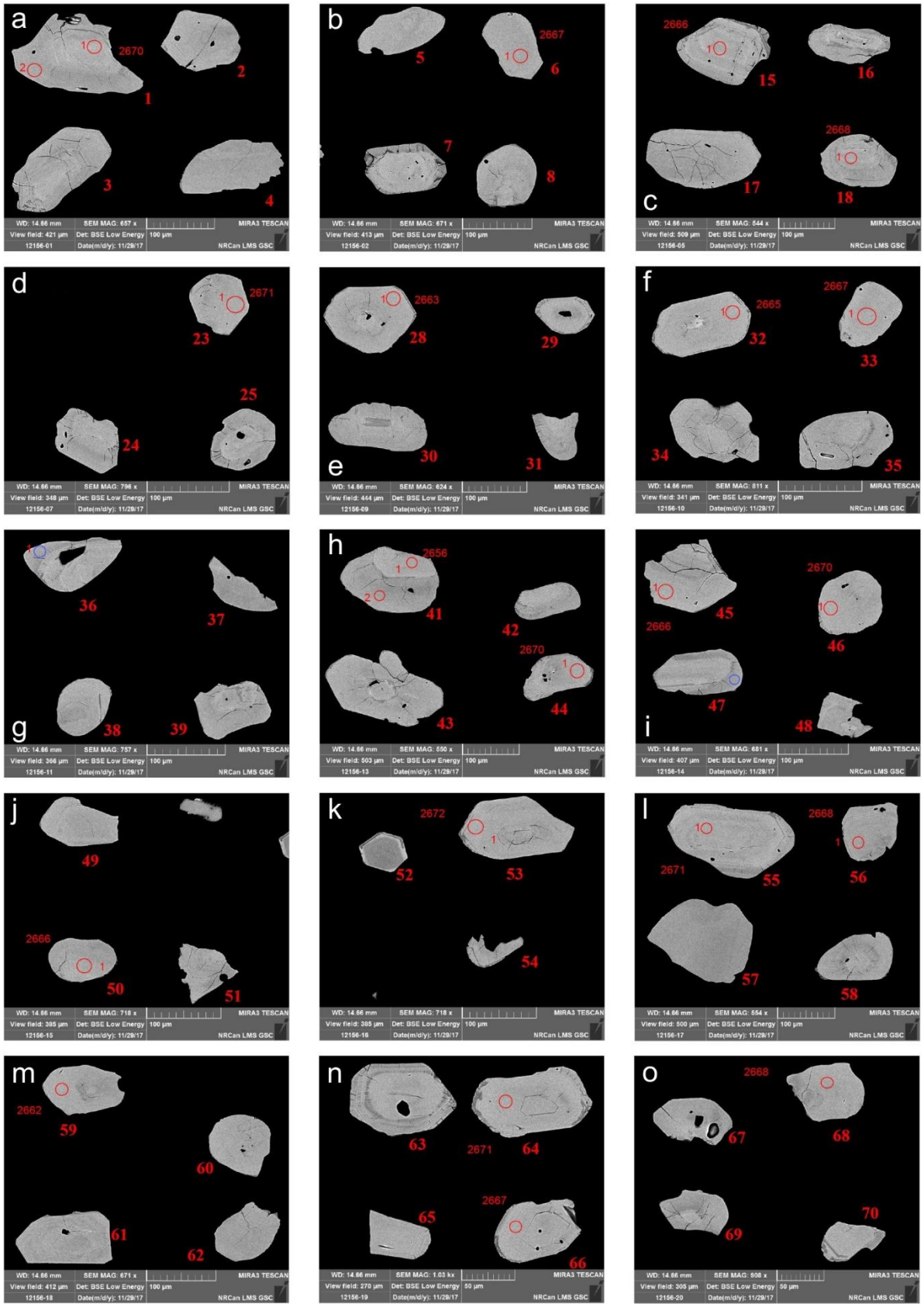

Figure 5.3: SEM BSE images of zircons analyzed from sample KJM095. Location of spot analyses indicated by red and blue circles with $^{207}Pb/^{206}Pb$ ages beside them.

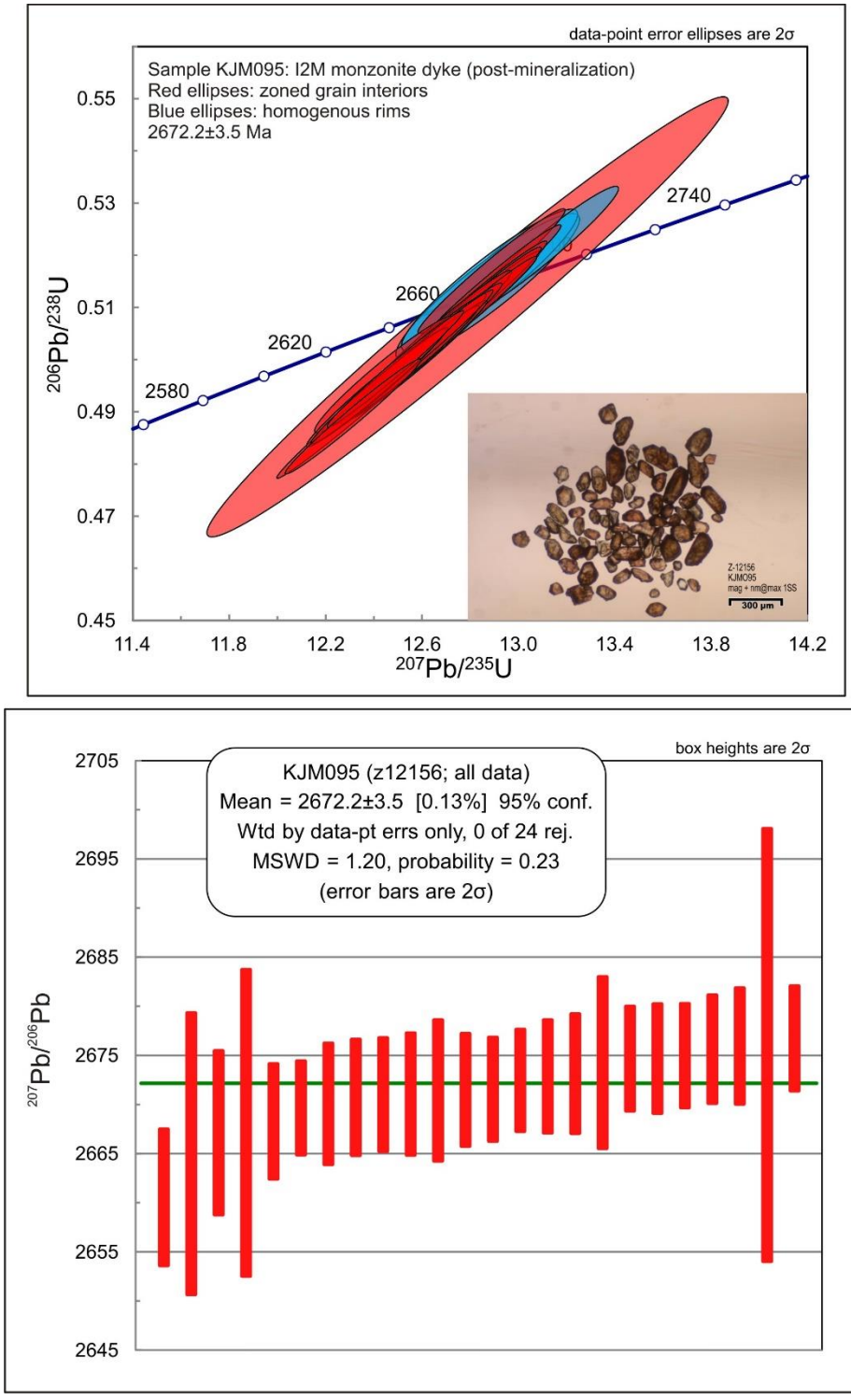

Figure 5.4: Concordia diagram and weighted average diagram showing data for sample KJM095 from the I2M intrusion. Inset image shows zircon population after mineral separation.

6. Summary and Discussion

6.1 Summary

6.1.1 Generations of deformation

Three generations of deformation were identified and characterized within the study area (Figure 6.1). D1 deformation occurred during regional compression and resulted in the development of large-scale F1 folds and the associated axial plane of S1 cleavage. During deformation, the Webb Lake Stock was intruded along a parasitic, camp-scale F1 fold within the study area.

D2 deformation occurred during north-side-up transpression and regional greenschist-grade metamorphism. The sinistral Goudreau Lake Deformation Zone formed during D2 deformation, with associated S2 foliation developing sub-parallel to the deformation zone and average L2a stretching lineation plunging along the axis of elongation. The main Island Gold deposit was also emplaced during D2 deformation, in zones sub-parallel to S2 foliation and the deformation zone.

D3 deformation occurred during south-side-up transpression and resulted in the development of F3 folds with associated axial-planar S3 cleavage. D3 deformation folded and sheared D2 structures to varying degrees. The extent of overprinting appears to be dependent on the hosting lithology as well as the presence or absence of intrusions.

6.1.2 Vein sets

Four vein sets were identified at the Island Gold deposit based on composition and overprinting relationships. They were documented through underground mapping of mining drifts and structural measurements.

V_{GD} veins are gold-bearing, sub-horizontal extensional quartz veins that are tightly folded into upright, shallowly plunging folds. They are found in the Goudreau zone and are hosted by both dacitic volcanics and trondhjemitic intrusive bodies.

V1 veins are gold-bearing, smoky grey laminated quartz shear veins that dip steeply to the south, sub-parallel to S2 foliation. Visible gold is common in V1 veins and occurs as both droplets and clouds within the quartz and along slip faces. V1 veins are present in the Goudreau Zone but are best developed in the Island zones and carry the majority of mineralization at the Island Gold deposit. They were emplaced along C-surfaces within the southern high strain zone, during the formation of the Goudreau Lake Deformation Zone and D2 deformation.

V2 veins are mineralized crack-seal quartz veinlets that occur sub-parallel to V1 veins and mimic S2 foliation. They carry subsidiary mineralization and often contain sericite and chlorite. V2 veins are considered to be broadly contemporaneous with V1 veins.

V3 veins are barren to weakly mineralized quartz-carbonate extensional veins that cross-cut the ore zones. They often appear as boudin-necks within V1 veins in drift faces, but also occur as shallowly south-dipping extensional veins and as en echelon veins. V3 veins were emplaced in extensional fractures during D3 deformation.

V4+ veins are barren tourmaline veins that overprint all pre-existing vein sets and fabrics.

6.1.3 U-Pb dating

Sample SH-3 was taken from the Webb Lake Stock, a mineralized trondhjemitic intrusion to the northwest of the Island Gold deposit which intruded along the F1 fold axial plane during D1 deformation. The sample returned a weighted mean $^{207}Pb/^{206}Pb$ age of 2724.1±4.3 Ma, which places an older limit on the absolute timing of mineralization as well as an approximate timing of D1 deformation.

Sample KJM095 was taken from the "I2M", a barren foid-bearing monzonite intrusion which cross-cuts the Island ore zones at depth. The sample returned a weighted mean $^{207}Pb/^{206}Pb$ age of 2672.2±3.5 Ma, which places a younger limit on the absolute timing of mineralization as well as D2 deformation.

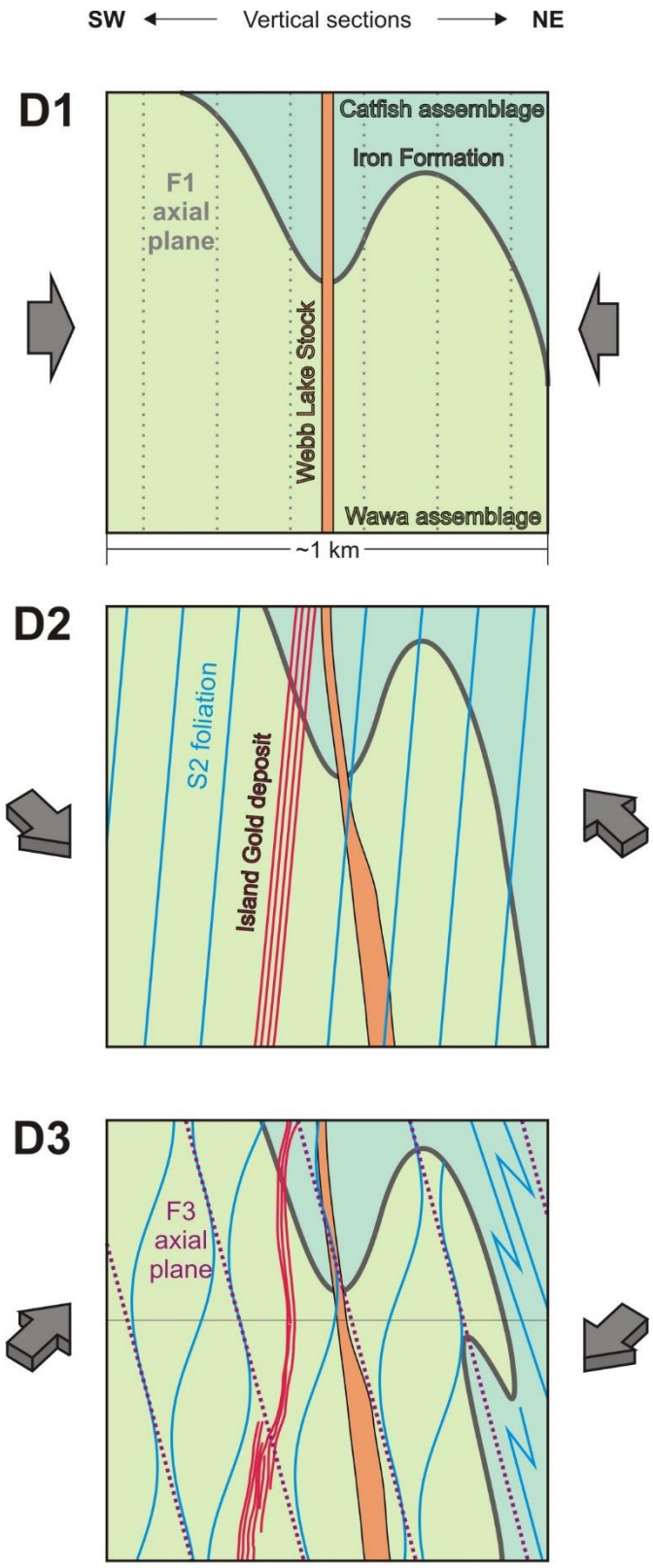

Figure 6.1: Schematic diagram showing the development of structures during D1-3 deformation in the study area. Grey arrows represent principle shortening axes during progressive D1-3 deformation. Horizontal grey line in lowest block represents current surficial expression.

6.2 Timing of mineralization

6.2.1 Island Gold deposit

Ages obtained from U-Pb geochronology are combined with field relationships to provide constraints on the timing of mineralization. Zircon analyses from the trondhjemitic Webb Lake Stock give a weighted mean $^{207}Pb/^{206}Pb$ age of 2724.1±4.3 Ma. This agrees within error with the 2722±1 Ma U-Pb age of the trondhjemitic Gutcher Lake Stock (Turek et al., 1984) and they can be considered broadly consanguineous. The amphibolite-grade, contact-metamorphism aureole that surrounds the Gutcher Lake Stock has been overprinted by regional greenschist-facies metamorphism (Sage, 1994), and gold mineralization in and surrounding the Gutcher Lake Stock has been correlated to greenschist-facies minerals (Studemeister, 1983). This overprinting relationship, combined with the structurally-controlled emplacement of the Webb Lake Stock along the axial plane of an F1 fold, indicate that both stocks were emplaced during D1 deformation. Emplacement of V1 veins and associated mineralization occurred during regional greenschist-facies metamorphism which postdated the emplacement of the stocks and as such is interpreted to have occurred during D2 deformation. The age obtained from the Webb Lake Stock therefore places the absolute timing for ongoing D1 deformation and an older age limit on mineralization at 2724.1±4.3 Ma.

Zircon analyses from the barren "I2M" cross-cutting intrusion returned a weighted mean $^{207}Pb/^{206}Pb$ age of 2672.2±3.5 Ma, which places it in the range of a regional plutonic event. Included in this event are the 2671±2 Ma Maskinonge Lake granodiorite and Troupe Lake quartz-monzonite stocks (Corfu and Sage, 1992) which lie to the north and northeast, respectively, of the study area and show only minor

development of tectonic fabrics (Turek *et al.*, 1996). Amphibolite-grade contact metamorphism surrounding the Troupe Lake Stock grades to the regional greenschist-facies level of metamorphism (Sage, 1993), indicating that it was emplaced late during or after regional metamorphism. The lack of mineralization within the "I2M" intrusion, the cross-cutting relationship with the Island Gold ore zones, and the metamorphic field relationships of contemporaneous stocks indicate that the "I2M" intrusion was emplaced post-mineralization and post-regional greenschist-facies metamorphism. It is therefore interpreted that the age obtained from the "I2M" intrusion places an absolute youngest age limit at 2672.2±3.5 Ma for the end of D2 deformation and associated regional greenschist-facies metamorphism and mineralization.

The age of the northern Doré metasedimentary rocks, which were affected by greenschist-facies metamorphism, is constrained to ≤2680±3 Ma (Corfu & Sage, 1992), the age of the youngest detrital zircon dated. Regional greenschist-facies metamorphism occurred during D2 deformation, indicating that D2 deformation was ongoing during or began shortly after the deposition of the Doré metasediments. The Island Gold deposit was emplaced during D2 deformation, and the above age constraints indicate that mineralization most likely took place between 2680±3 Ma and 2672.2±3.5 Ma.

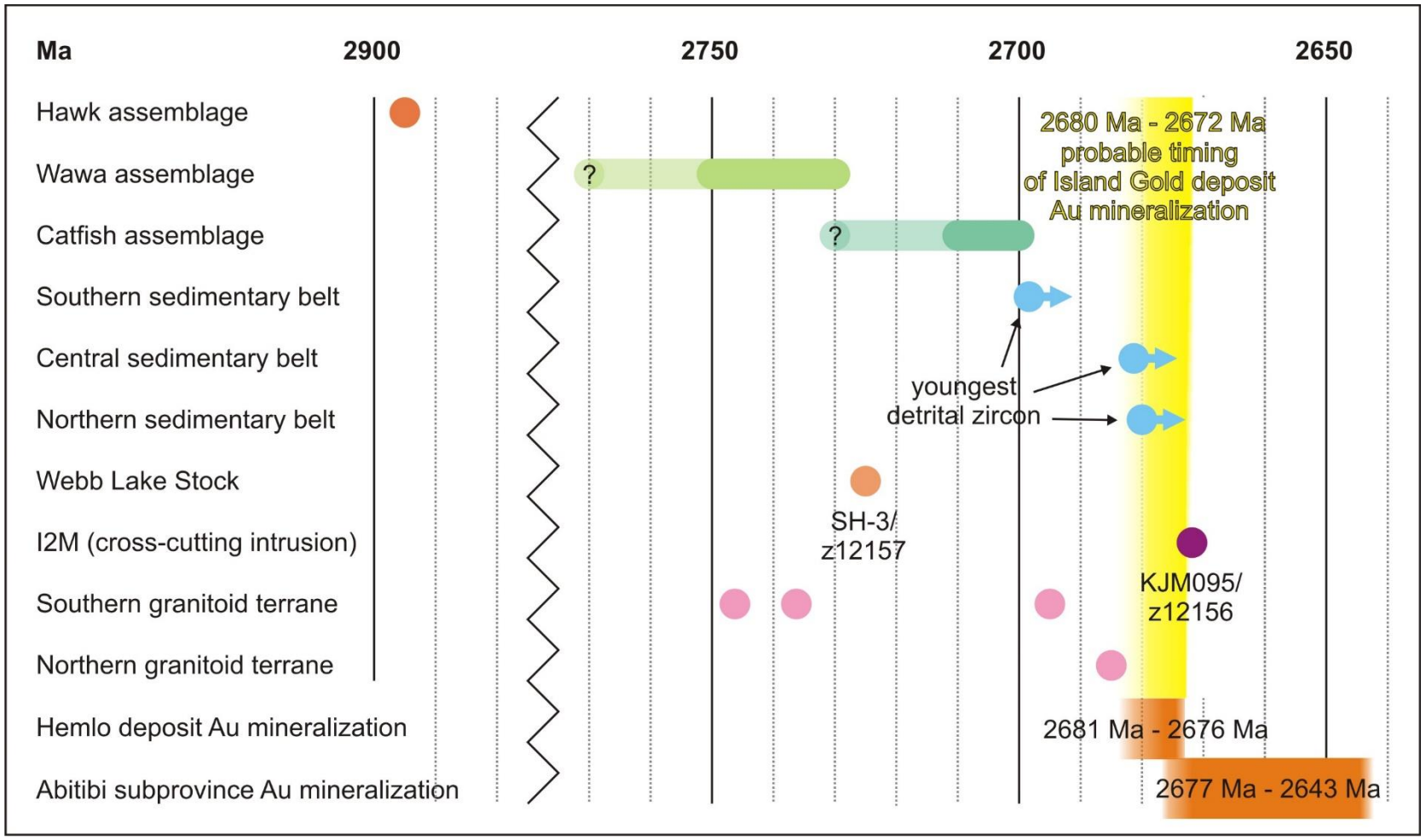

Figure 6.2: Geochronological diagram summarizing U-Pb constraints on mineralization at the Island Gold deposit. Michipicoten greenstone belt ages from Turek et al. (1984, 1992); Corfu & Sage (1992); and this study, Hemlo deposit ages from Davis & Lin (2003), and Abitibi subprovince ages from Beakhouse (2007).

6.3 Structural control on mineralization

Competency contrast controls the Goudreau Lake Deformation Zone and Island Gold deposit at multiple scales.

6.3.1 Goudreau Lake Deformation Zone

Most workers in the Michipicoten greenstone belt have cited the competency contrast between two volcanic assemblages as the main regional control on the concentration of strain and subsequent formation of the regional Cradle Lake and Goudreau Lake Deformation Zones (Heather and Arias, 1992; Sage, 1994). A previous hypothesis also postulated that the intrusions along the northern edge of the belt helped to further concentrate strain, however with recent U-Pb ages (this study) that constrain the timing of mineralization to pre-northern intrusions, this is unlikely. The Goudreau Lake Deformation Zone is centred at, and is widest at, the contact between the felsic to intermediate rocks of the upper Wawa assemblage and the mafic to intermediate rocks of the lower Catfish assemblage (Figure 2.4). It is therefore likely that concentration of strain and formation of the Goudreau Lake Deformation Zone is a function of the competency contrast present at the contact which occurred at a sympathetic angle to ongoing deformation.

6.3.2 Island Gold deposit

Work within the northern domain of the Goudreau Lake Deformation Zone identifies a large mafic meta-intrusive sheet that is interpreted to have provided competency contrast and focused strain to produce the Kremzar and similar-type deposits (Heather and Arias, 1992). In the southern domain of the deformation zone the Webb Lake Stock also provides competency contrast, and gold showings do occur within

and around the intrusion, but the largest of these occurrences (the Island Gold deposit) is located at a distance from the intrusion (Figure 3.1). The southern domain of the Goudreau Lake Deformation Zone is the only domain hosted by felsic to intermediate volcanic rocks and displays a deformation style that is unique from the other domains. Although there are some similarities between mineralization style in the northern and southern domains, the Island Gold deposit is unique in its economic grade and geometry.

Here, a model for the emplacement of the Island Gold deposit is proposed that takes into consideration the previously outlined deformation history of the Goudreau Lake Deformation Zone, as well as the associated generations of vein sets and the geometry of the deposit. Within the Goudreau Lake Deformation Zone, the Webb Lake Stock behaved more competently than the surrounding volcanics and strain was consequently further concentrated along the edges of the stock, creating high-strain zones along the north and south flanks. Minor mineralization is hosted by the northern high-strain zone, but the highest-grade and most continuous is hosted by the southern high-strain zone, at the Island Gold deposit. The Island Gold deposit occurs at a small angle to, and approximately 250m southeast of, the Webb Lake Stock. The geometry of the Webb Lock Stock creates a protruding edge along the southern flank, and the Island Gold deposit is located northeast along strike of S2 foliation from this edge (Figure 6.3). The majority of mineralization in the Island Gold deposit is carried by V1 shear veins, which were emplaced sub-parallel to S2 foliation during D2 deformation. Movement during D2 deformation was sinistral, north-side-up transpression which, when applied to the geometry of the Webb Lake Stock, created a strain shadow to the east and down-

dip of the protruding edge along the southern flank of the stock. The dilation necessary for the emplacement of V1 shear veins was facilitated by a releasing band along the edge of the strain shadow created by the Webb Lake Stock.

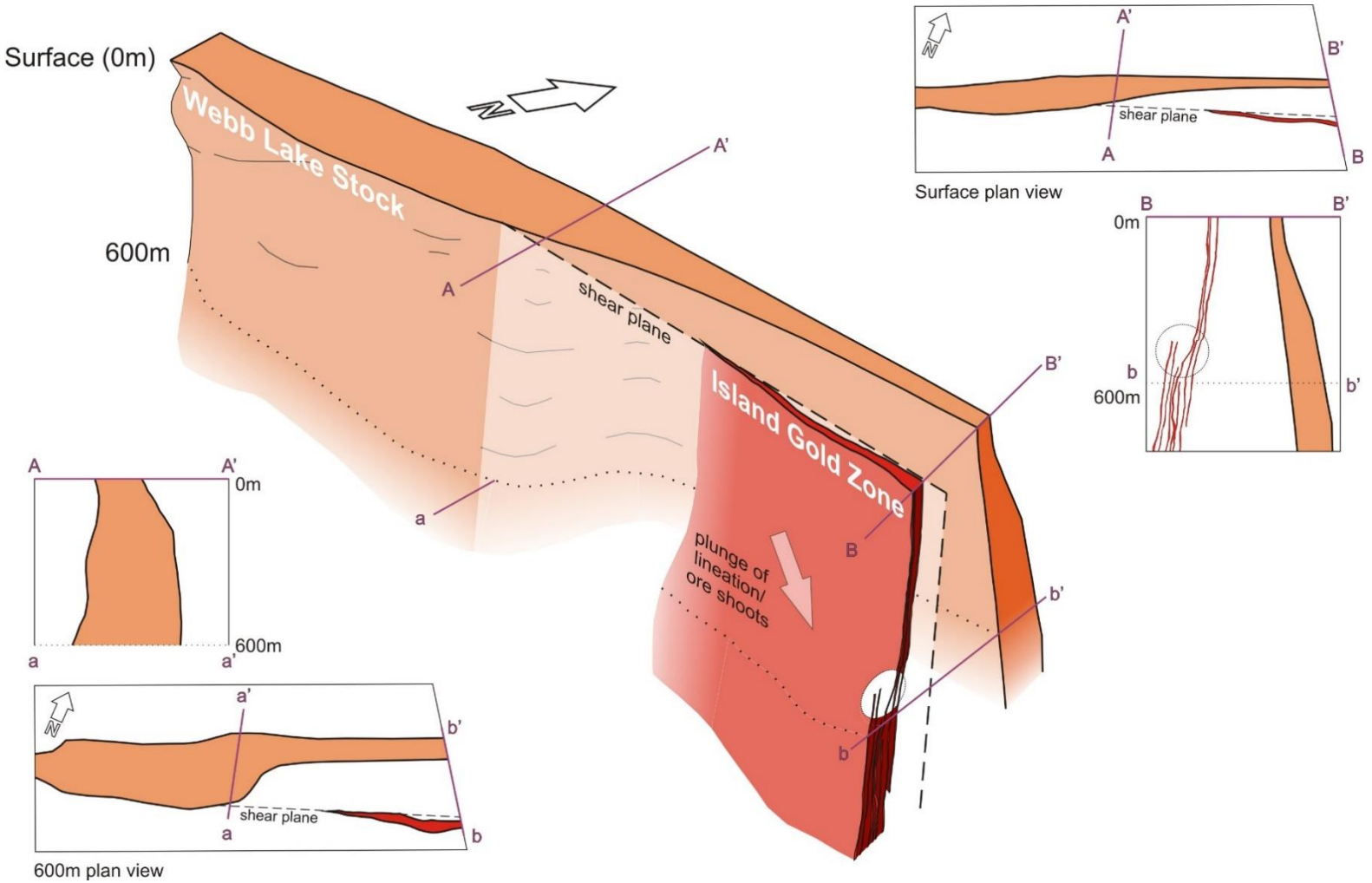

Figure 6.3: Orthographic projection schematically showing the three-dimensional geometry of the Island Gold deposit and the Webb Lake Stock with horizontal and vertical sections. Looking down toward northwest, except where indicated. Note how the Island Gold Zone lies along the shear plane that extends from a protrusion in the Webb Lake Stock.

7. Conclusions and Future Work

7.1 Conclusions

The main conclusions from this research are as follows:

1. Formation of the Goudreau Lake Deformation Zone was controlled by the competency contrast between volcanic packages;
2. Island Gold ore veins were emplaced sub-parallel to S_2 foliation in the Goudreau Lake Deformation Zone during D_2 deformation;
3. Timing of mineralization is constrained to between ≤2680 Ma and 2672 Ma; and
4. The Webb Lake Stock created a strain shadow, facilitating the emplacement of the Island Gold deposit.

7.2 Future work

The main structural controls on the Island Gold deposit have been documented by this thesis, but further work is required to gain a better understanding of the following:

1. The I2H ("C-zone dyke") is a highly altered and deformed intrusion which is observed coincident to the main economic ore zone in the Island and Island Deep Zones, the C-zone. While the I2H appears to cross-cut the ore zone and is not mineralized, it has not been definitively proven to be emplaced post-mineralization. Given its association with the C-zone, further study into the timing of emplacement and potential influence on mineralization is needed.
2. The Goudreau Zone appears to be distinct from the main Island and Extension Zones and may represent a separate mineralization or remobilization event. Further investigation into the structural (or other) controls on mineralization and the timing of mineralization relative to the Island and Extension Zones is necessary to determine how the Goudreau Zone fits into the overall geologic model of the Island Gold deposit.

References

Arias, Z.G. and Heather, K.B. 1987. Regional structural geology related to gold mineralization in the Goudreau-Lochalsh area, District of Algoma; Summary of Field Work and Other Activities, Ontario Geological Survey, Miscellaneous Paper 137, p. 146-154

Arias, Z.G. and Helmstaedt, H. 1990. Structural evolution of the Michpicoten (Wawa) greenstone belt, Superior Province: evidence for an Archean fold and thrust belt; Geoscience Research Grant Program, Summary of Research 1989-1990, Ontario Geological Survey, Miscellaneous Paper 150, p. 107-114.

Beakhouse, G.P. 2007. Structurally controlled, magmatic hydrothermal model for Archean lode gold deposits: a working hypothesis; Ontario Geological Survey, Open File report 6193, 133 p.

Bruce, E.L., 1940. Geology of the Goudreau-Lochalsh area; Ontario Department of Mines, Annual Report, v. 49, Part 3, p. 50.

Card, K.D. 1990. A review of the Superior Province of the Canadian Shield, a product of Archean accretion; Precambrian Research, v. 48, p. 99-156.

Ciufo, T. 2019. Hydrothermal Alteration and Exploration Vectors at the Orogenic Island Gold Deposit, Michipicoten greenstone belt, Wawa, Ontario; MSc thesis, University of Waterloo, 344 p.

Corfu, F. and Sage, R.P. 1992. U-Pb age constraints for the deposition of clastic metasedimentary rocks and late-tectonic plutonism, Michipicoten Belt, Superior Province; Canadian Journal of Earth Sciences, v. 29, p. 1640-1651.

Davis, D.W. and Lin, S. 2003. Unraveling the geologic history of the Hemlo Archean gold deposit, Superior Province, Canada: a U-Pb geochronological study; Economic Geology, v. 98, p. 51-67.

Fossen, H., Tikoff, B. and Teyssier, C. 1994. Strain Modeling of transpressional and transtensional deformation; Norsk Geologisk Tidsskrift, v. 74(3), p. 134.145.

Goodwin, A.M. 1962. Structure, stratigraphy, and origin of iron formations, Michipicoten area, Algoma district, Ontario, Canada; Geological Society of America Bulletin, v. 73, p. 561-586.

Goodwin, A.M. 1964. Geochemical studies at the Helen Iron Range; Economic Geology, v. 59, p. 684-718.

Heather, K.B. and Arias, Z.G. 1987. Geological setting of gold mineralization in the Goudreau-Lochalsh area, District of Algoma; Summary of Field Work and Other Activities, Ontario Geological Survey, Miscellaneous Paper 137, p. 155-162

Heather, K.B. and Arias, Z.G. 1992. Geological and structural setting of gold mineralization in the Goudreau-Lochalsh area, Wawa gold camp; Ontario Geological Survey, Open File Report 5832, 159 p.

Lin, S. and Beakhouse, G.P. 2013. Synchronous vertical and horizontal tectonism at late stages of Archean cratonization and genesis of Hemlo gold deposit, Superior craton, Ontario, Canada; GEOLOGY, v. 41, p. 359-362.

Lin, S., Jiang, D., and Williams, P.F. 1998. Transpression (or transtension) zones of triclinic symmetry: natural example and theoretical modelling; Geological Society, London, Special Publications, v. 135, p. 41-57.

Ludwig, K.R., 2008. User's manual for Isoplot 3.70: A Geochronological Toolkit for Microsoft Excel; Berkeley Geochronology Center Special Publication No. 4, rev. August 26, 2008, 76 p.

McGill, G.E. 1992. Structure and kinematics of a major tectonic contact, Michipicotem greenstone belt, Ontario; Canadian Journal of Earth Sciences, v. 29, p. 2118-2132.

McGill, G.E. and Shrady, C.H. 1988. Structure of southwestern Michipicoten greenstone belt, Ontario: evidence for Archean accretion?; Workshop on the Growth of Continental Crust, p. 98.

Percival, J.A., Sanborn-Barrie, M., Skulski, T., Stott, G.M., Helmstaedt, H. and White, D.J. 2006. Tectonic evolution of the western Superior Province from NATMAP and Lithoprobe studies; Canadian Journal of Earth Sciences, v. 43, p. 1085-1117.

Percival, J.A., Skulski, T., Sanborn-Barrie, M., Stott, G.M., Leclair, A.D., Corkery, M.T., and Boily, M. 2012. Geology and tectonic evolution of the Superior Province, Canada. Chapter 6 *In* Tectonic Styles in Canada: The LITHOPROBE Perspective, Geological Association of Canada, Special Paper 49, p. 321–378.

Rice, R.J. and Donaldson, J.A. 1992. Sedimentology of the Archean Doré metasediments, Arliss Lake area, southern Michipicoten greenstone belt, Superior Province; Canadian Journal of Earth Sciences, v. 29, p. 2558-2570.

Sage, R.P. 1987. Geology of the Goudreau-Lochalsh and Kabenung Lake areas, District of Algoma; Summary of Field Work and Other Activities, Ontario Geological Survey, Miscellaneous Paper 137, p.134-137.

Sage, R.P. 1993. Geology of Agounie, Bird, Finan and Jacobson townships, District of Algoma; Ontario Geological Survey, Open File Report 5588, 286 p.

Sage, R.P. 1994. Geology of the Michipicoten greenstone belt; Ontario Geological Survey, Open File Report 5888, 592 p.

Smith, P.E. 1981. Rb-Sr whole rock and U-Pb zircon geochronology of the Michipicoten greenstone belt, Wawa area, northwestern Ontario; MSc thesis, University of Windsor, Windsor ON.

Stern, R.A. 1997. The GSC Sensitive High Resolution Ion Microprobe (SHRIMP): analytical techniques of zircon U-Th-Pb age determinations and performance evaluation: in Radiogenic Age and Isotopic Studies, Report 10, Geological Survey of Canada, Current Research 1997-F, p. 1-31.

Stern, R.A., and Amelin, Y. 2003. Assessment of errors in SIMS zircon U-PB geochronology using a natural zircon standard and NIST SRM 610 glass; Chemical Geology, v. 197, p. 111-146.

Studemeister, P.A. 1983. The greenschist facies of an Archean assemblage near Wawa, Ontario; Canadian Journal of Earth Sciences, v. 20, p. 1409-1420.

Sylvester, P.J., Attoh, K., and Schulz, K.J. 1987. Tectonic setting of late Archean bimodal volcanism in the Michipicoten (Wawa) greenstone belt, Ontario; Canadian Journal of Earth Sciences, v. 24, p. 1120-1134.

Tikoff, B. and Greene, D. 1996. Stretching lineations in transpressional shear zones: an example from the Sierra Nevada Batholith, California; Journal of Structural Geology, v. 19, p. 29-39.

Turek, A. and Van Schmus, W.R. 1982. Rb-Sr and U-Pb ages of volcanism and granite emplacement in the Michipicoten belt – Wawa, Ontario; Canadian Journal of Earth Sciences, v. 19, p. 1608-1626.

Turek, A., Smith, P.E. and Van Schmus, W.R. 1984. U-Pb zircon ages and the evolution of the Michipicoten plutonic-volcanic terrane of the Superior Province, Ontario; Canadian Journal of Earth Sciences, v. 21, p. 457-464.

Turek, A., Keller, R. and Van Schmus, W.R. 1990. U-Pb zircon ages of volcanism and plutonism in the Mishibishu greenstone belt near Wawa, Ontario; Canadian Journal of Earth Sciences, v. 27, p. 649-656.

Turek, A., Sage, R.P. and Van Schmus, W.R. 1992. Advances in the U-Pb zircon geochronology of the Michipicoten greenstone belt, Superior Province, Ontario; Canadian Journal of Earth Sciences, v. 29, p. 1154-1165.

Turek, A., Heather, K.B., Sage, R.P. and Van Schmus, W.R. 1996. U-Pb zircon ages for the Missanabie-Renabie area and their relation to the rest of the Michipicoten greenstone belt, Superior Province, Ontario, Canada; Precambrian Research, v. 76, p. 191-211.

Williams, H.R., Stott, G.M., Heather, K.B., Muir, T.L., and Sage, R.P. 1991. Wawa Subprovince; *in* Geology of Ontario, Ontario Geological Survey, Special Volume 4, Part I, p. 485-539.